# An hybrid Approach for the Computation of Guided Modes in Integrated Optics

A. Bermudez, Gómez Pedreira, Patrick Joly

INRIA

INSTITUT NATIONAL DE RECHERCHE EN INFORMATIQUE ET EN AUTOMATIQUE

# *An hybrid approach for the computation of guided modes in integrated optics*

A. Bermúdez, D. Gómez Pedreira and P. Joly

**N ° 4148**

Mars 2001

THÈME 4


ISSN 0249-6399 ISRN INRIA/RR--4148--FR+ENG

INRIA
ROCQUENCOURT

# An hybrid approach for the computation of guided modes in integrated optics

A. Bermúdez, D. Gómez Pedreira and P. Joly*

Thème 4 — Simulation et optimisation
de systèmes complexes
Projet Ondes

Rapport de recherche n°4148 —Mars 2001 — 43 pages

**Abstract:** In this work, we are interested in the numerical approximation of an eigenvalue problem posed in $\mathbb{R}^2$ arising from the computation of guided modes in integrated optics waveguides, which are particular cases of open waveguides.

We consider a stratified waveguide translationally invariant in the infinite propagation direction. Its cross-section is also supposed to be an unbounded and stratified medium where an appropiate perturbation of the refraction index has been introduced to ensure the existence of guided modes.

Under the weak guiding assumption, a method to compute the guided modes has been proposed and analyzed in [11]. This method appears as a combination of analytical methods which take into account the unbounded and stratified character of the propagation medium and numerical computations which can be reduced to a neighborhood of the perturbation.

In this paper, we are concerned with the numerical implementation of the method and we present some numerical results.

**Key-words:** Integrated optics, guided modes, open electromagnetic waveguides, numerical methods, mixed elements, hybrid methods.

*(Résumé : tsvp)*

* mabermud@usc.es, malola@usc.es, Patrick.Joly@inria.fr

Unit´e de recherche INRIA Rocquencourt
Domaine de Voluceau, Rocquencourt, BP 105, 78153 LE CHESNAY Cedex (France)
T´el´ephone : 01 39 63 55 11 - International : +33 1 39 63 55 11
T´el´ecopie : (33) 01 39 63 53 30 - International : +33 1 39 63 53 30

# Une méthode hybride pour le calcul d'ondes guidées en optique intégrée

**Résumé :** Dans ce rapport, nous nous interessons á l'approximation numérique d'un problème de valeurs propres en milieu non borné pour un opérateur différentiel de second ordre. Ce type de problème apparaît dans le calcul d'ondes électromagnétiques guidées en optique intégrée, dans le cadre de l'hypothèse du faible guidage.

Nous considérons un guide ouvert invariant par translation dans une direction et occupant tout l'espace $\mathbb{R}^3$. La section transverse du guide apparaît comme une perturbation locale d'un milieu stratifié et on fait l'hypothèse que la distribution de l'indice de réfraction est telle que des modes guidés existent.

Dans [11] nous avons présenté et analysé une méthode pour le calcul des modes guidés qui apparaît comme une combinaison de méthodes analytiques pour la prise en compte du milieu non perturbé et de méthodes numériques pour la prise en compte de la perturbation.

Dans ce travail, nous nous interessons á l'implementation numérique de cette méthode et nous presentons quelques resultats numériques.

**Mots-clé :** Modes guidés, ondes électromagnétiques, optique integrée, méthodes numériques, éléments mixtes, méthodes hybrides.

# Contents

# 1 Introduction

In this work, we are interested in the numerical approximation of an eigenvalue problem posed in $\mathbb{R}^2$ arising from the computation of guided modes in integrated optics waveguides which are particular cases of open waveguides.

Open waveguides are propagation structures which are supposed to be invariant with respect both to the geometry and to its physical characteristics under any translation along one privileged space direction, let us say $x_3$, which coincides with the infinite propagation direction of the waves. In particular, the refraction index $n$ of the waveguide will depend only on the two transverse coordinates $x = (x_1, x_2)$ of the cross section of the guide. The function $n(x)$ coincides with the refraction index $\bar{n}(x)$ of a *simple reference* medium outside a bounded region $\mathcal{K}$ of the $(x_1, x_2)$ plane whose dimensions are so small that, from the mathematical point of view, the cross section of the guide is considered as an unbounded domain. This is why we speak of an *open* waveguide.

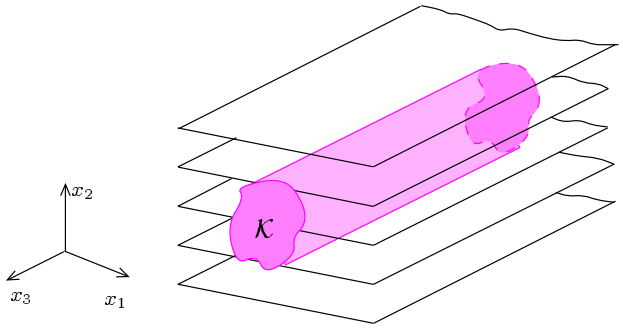


Figure 1: Sketch of an open stratified waveguide and the choice of the coordinate system.

An optical fiber is an open waveguide for which the reference medium is homogeneous: $\bar{n}$ is constant. The specificity of an integrated optics waveguide lies in the fact that the reference medium is heterogeneous but stratified: $\bar{n}$ only depends of one space variable, $x_2$ for instance. If the materials composing the different layers are chosen with a suitable refraction index, then the energy of the wave can be vertically confined in the material with the largest index. But it is the distribution of the refraction index inside the region $\mathcal{K}$ which, if chosen properly (see [3], [12]), allows harmonic electromagnetic waves of finite transverse energy to propagate without attenuation along the device. These waves are called *guided modes* (or *guided waves*)

and are particular solutions of Maxwell's equations of the form

$$\begin{aligned} \mathbf{E}(x, x_3, t) &= \mathbb{E}(x)\, e^{i(\omega t - \beta x_3)}, \\ \mathbf{H}(x, x_3, t) &= \mathbb{H}(x)\, e^{i(\omega t - \beta x_3)}, \end{aligned} \tag{1.1}$$

where

- $\omega > 0$ is the *angular frequency* (or *pulsation*) of the wave,
- $\beta > 0$ is the *wavenumber* (or *propagation constant*) of the mode,
- $\mathbb{E}(x) = (E_1(x), E_2(x), E_3(x))$ and $\mathbb{H}(x) = (H_1(x), H_2(x), H_3(x))$ are 2D vector fields describing the distribution of the electromagnetic field in each cross section, that must satisfy the *finite transverse energy* condition

$$\int_{\mathbb{R}^2} (|\mathbb{E}|^2 + |\mathbb{H}|^2)\, dx < \infty. \tag{1.2}$$

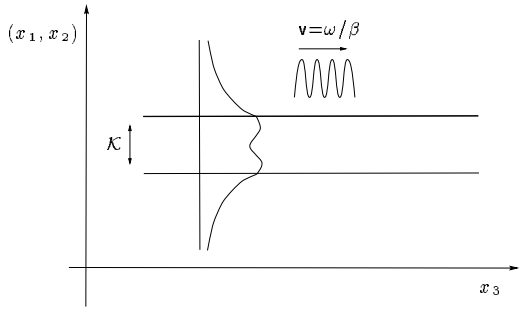


Figure 2: Structure of a guided wave. v denotes the phase velocity.

Such solutions are the ones we are interested to compute. Although the exact model (Maxwell's equations) is vectorial, one can show that, under the *weak guidance* assumption (see [2] and [19]), that is, large wavenumber and weak variations of the refraction index, the searching of guided waves can be reduced to the following scalar problem

$$(\mathcal{P}) \quad \left\{ \begin{array}{l} \textit{Find } \omega > 0, \beta > 0 \textit{ and } \quad u \in \mathrm{L}^2(\mathbb{R}^2) \quad (u \neq 0) \textit{ such that} \\ -\Delta\, u + \beta^2\, u = \omega^2\, n^2\, u\,, \end{array} \right. \tag{1.3}$$

where $u$ denotes any of the transverse components $E_1(x), E_2(x), H_1(x)$ or $H_2(x)$ of the electric or magnetic field.

The question we address in this paper is to solve numerically problem $(\mathcal{P})$. This problem can be considered in two ways (the second one being physically more relevant):

- Given the propagation constant $\beta$ and the refraction index distribution $n(x)$, find the pulsation $\omega$ and the transverse field $u(x)$.
- Given the pulsation $\omega$ and the refraction index distribution $n(x)$, find the propagation constant $\beta$ and the transverse field $u(x)$.

The relationship between $\omega$ and $\beta$ characterizes what is called the *dispersion* of the mode.

In each case, one has to solve a self-adjoint eigenvalue problem in an unbounded and stratified domain, which makes the numerical solution non trivial. We will adopt here the first option, however this choice has no real influence on our numerical method. Thus, we will be interested in computing the guided modes associated to eigenvalues $\omega^2$ in the discrete spectrum of the operator $\mathcal{A}_\beta = n^{-2}(-\Delta + \beta^2)$, assuming they exist (see [3] and [12] for existence conditions). These eigenvalues satisfy (see [11, 9])

$$\beta^2/n_+^2 < \omega^2 < \sigma_e(\beta), \tag{1.4}$$

where

$$n_+ = \sup_{x\in\mathbb{R}^2} n(x)$$

and $\sigma_e(\beta)$ denotes the greatest lower bound of the essential spectrum of the operator $\mathcal{A}_\beta$. We shall denote

$$E = \{(\omega,\beta) \in \mathbb{R}^2 \,/\, \omega > 0,\ \beta > 0,\ \beta^2/n_+^2 < \omega^2 < \sigma_e(\beta)\ \}.$$

The typical situation is the following: for a given value of $\beta$, $\mathcal{A}_\beta$ has a finite number of eigenvalues $\{\omega_j^2(\beta), 1 \le j \le \mathcal{N}_\beta\}$. The number $\mathcal{N}_\beta$ may vary with $\beta$ and $\mathcal{N}^\star = \sup \mathcal{N}_\beta$ can be infinite. For any $j \le \mathcal{N}^\star$, the $j$th eigenvalue $\omega_j^2(\beta)$ exists for an interval $[\beta_j^-, \beta_j^+]$ of values of $\beta$, $0 \le \beta_j^- < \beta_j^+ \le +\infty$. $\beta_j^-$ (respectively $\beta_j^+$) is called the lower (respectively upper) *threshold* or *cut-off* wave number for the $j$th guided mode. In a lot of situations $\beta_j^+ = +\infty$.

- When $\beta \searrow \beta_j^-$, $\omega_j(\beta) \to \sigma_e(\beta)$ and the corresponding eigenfunction is less and less confined.
- If $\beta_j^+ = +\infty$, when $\beta \nearrow +\infty$, the corresponding eigenfunction is more and more confined in the layer $\Omega_i$.

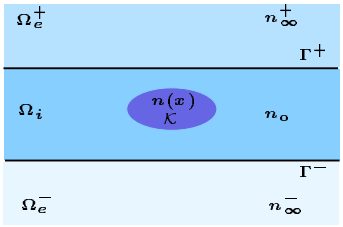


Figure 3: Cross section with three different layers.

**Remark 1.1** *Although, in particular situations, eigenvalues embedded in the essential spectrum may exist (see* [4]*) there is a conjecture that the set of embedded eigenvalues is "generically" empty. Such modes are thus very unstable with respect to the physical imperfections of the guide and then not so interesting from a practical point of view.*

In the sequel, we shall reduce ourselves to a three layer reference medium corresponding to (see Fig. 3)

$$\bar{n}(x_2) = \begin{cases} n_\infty^- & \text{if} \quad x_2 \in \Omega_e^- = \{(x_1, x_2) \in \mathbb{R}^2,\ x_2 < 0\}, \\ n_o & \text{if} \quad x_2 \in \Omega_i = \{(x_1, x_2) \in \mathbb{R}^2,\ 0 < x_2 < L\}, \\ n_\infty^+ & \text{if} \quad x_2 \in \Omega_e^+ = \{(x_1, x_2) \in \mathbb{R}^2,\ x_2 > L\}, \end{cases}$$

where we can assume without loss of generality that $n_\infty^- \leq n_\infty^+$. We also assume that the perturbation $\mathcal{K}$ is included in the central layer $\Omega_i$. However, the numerical method we are going to present extends with minor modifications to the case where $n_o$ is a function of $x_2$, which includes the case of several homogeneous layers, even if the perturbation $\mathcal{K}$ is not completely embeded in one of them (see [12]).

Of course, the main difficulty amounts to reduce the effective calculations to a bounded domain in space and the geometry of the device makes impossible the use of classical artificial boundary conditions. For instance, for optical fibers, one can exploit separation of variables in polar coordinates outside a circle $S_R$ of radius $R$ enclosing the region $\mathcal{K}$ to write an exact Dirichlet to Neumann transparent condition on $S_R$ (see Bonnet [2], Joly and Poirier [13] or Givoli and Keller [8]). This is no longer possible in our case due to the stratified nature of the reference medium. Mahé [14] proposes an approximate method consisting in the introduction of two artificial

horizontal boundaries where a Dirichlet or Neumann condition is applied. The main drawback one can find in this method is that it is not exact: to get convergence to the true solution it is necessary to make the two horizontal boundaries go to infinity, which is very expensive numerically. It can also be expected that the accuracy of the results depends on frequency in the sense that this method will give very good results when the energy of the mode is very well confined in the vertical directions. On the contrary, we can expect a deterioration of the accuracy when $\beta$ is close to some cut-off wave number.

The method we propose in this work could be considered as an improvement of Mahé's method. It is based on a reformulation *at the boundary* of problem $(\mathcal{P})$. This new formulation, introduced in [11, 9], will be recalled in Section 2. Then, the outline of this paper is as follows. Section 3 is concerned with the numerical approximation of the problem. We will show how the domain of numerical computations can be reduced to a rectangle surrounding the perturbation. In Section 4, we propose a mixed-hybrid finite element method for numerical resolution in the rectangle and we write the problem in matrix form. Section 5 deals with the construction of the discrete operators appearing in the numerical approximation. Finally numerical results are given in Section 6.

## 2 A reformulation of the eigenvalue problem $(\mathcal{P})$

Let us introduce:

$$\Gamma^- = \{(x_1, 0),\ x_1 \in \mathbb{R}\} \quad (= \partial\Omega_e^-), \quad \Gamma^+ = \{(x_1, L),\ x_1 \in \mathbb{R}\} \quad (= \partial\Omega_e^+).$$

The idea is to formulate a problem whose unknown $\varphi = (\varphi^+, \varphi^-)$ is the trace of $u$ (the solution of $(\mathcal{P})$) on $\Gamma = \Gamma^+ \cup \Gamma^-$. For given $(\omega, \beta) \in E$, we introduce the operator $S(\omega, \beta)$ defined as follows (for the simplicity of the exposition, we omit to mention the appropriate functional framework and refer the reader to [11] for more details):

$$S(\omega, \beta)\,\varphi = \left[\frac{\partial u(\varphi)}{\partial \mathbf{n}}\right]_\Gamma = \left(\left[\frac{\partial u(\varphi)}{\partial \mathbf{n}}\right]_{\Gamma^+},\ \left[\frac{\partial u(\varphi)}{\partial \mathbf{n}}\right]_{\Gamma^-}\right), \tag{2.1}$$

where $u(\varphi)$ denotes the solution of the boundary value problem

$$(\mathcal{P}_\varphi) \quad \left\{ \begin{array}{rcll} -\Delta\, u(\varphi) \ + \ (\beta^2 - n^2\,\omega^2)\, u(\varphi) & = & 0 & \text{in} \quad \Omega = \mathbb{R}^2 \setminus \Gamma, \\ u(\varphi) & = & \varphi & \text{on} \quad \Gamma. \end{array} \right. \tag{2.2}$$

In (2.1), $\mathbf{n}$ denotes the outer unit normal vector to $\Gamma^+$ or $\Gamma^-$ and

$$[q]_\Gamma = ([q]_{\Gamma^+}, [q]_{\Gamma^-})$$

with

$$\begin{aligned} [q]_{\Gamma^+} &= (q|_{\Omega_i})|_{\Gamma^+} - (q|_{\Omega_e^+})|_{\Gamma^+}, \\ [q]_{\Gamma^-} &= (q|_{\Omega_i})|_{\Gamma^-} - (q|_{\Omega_e^-})|_{\Gamma^-}. \end{aligned}$$

The idea is the following: take a function $\varphi$ defined on $\Gamma$ and solve the boundary value problem $(\mathcal{P}_\varphi)$, (which consists, in fact, of two decoupled problems: one outside the strip $\Omega_i$ and another one inside). By construction, the function $u(\varphi)$ is continuous. In order that $u(\varphi)$ be a solution of problem $(\mathcal{P})$, it is enough to ensure the matching of the normal derivatives on the lines $x_2 = 0$ and $x_2 = L$: this means that the the jump of the normal derivative of $u(\varphi)$ across $\Gamma$, namely $S(\omega, \beta)\varphi$, must be equal to 0. Then, problem $(\mathcal{P})$ is equivalent to

$$(\mathcal{P}_S) \left\{ \begin{array}{c} \textit{For } \beta > 0, \textit{ find } \omega > 0 \textit{ with } (\omega, \beta) \in E \\ \textit{such that } 0 \textit{ is an eigenvalue of } S(\omega, \beta). \end{array} \right.$$

For numerical purposes, we use a decomposition of $S(\omega, \beta)$ into another three operators

$$S(\omega, \beta) = S_i(\omega, \beta) + S_p(\omega, \beta) - S_e(\omega, \beta) \tag{2.3}$$

which corresponds to a decomposition of $u$ as:

- $u|_{\Omega_e} = u_e^\pm$, with $u_e^\pm = u_e^\pm(\varphi)$ the unique solution of

$$(\mathcal{P}_e) \left\{ \begin{array}{rcll} -\Delta u_e^\pm + (\beta^2 - n_\infty^{\pm\,2}\,\omega^2)\, u_e^\pm &=& 0 & \text{in } \Omega_e^\pm, \\ u_e^\pm &=& \varphi & \text{on } \Gamma, \end{array} \right.$$

- $u|_{\Omega_i} = u_i + u_p$, with $u_i = u_i(\varphi)$ the unique solution of

$$(\mathcal{P}_i) \left\{ \begin{array}{rcll} -\Delta u_i + (\beta^2 - n_o^2\,\omega^2)\, u_i &=& 0 & \text{in } \Omega_i, \\ u_i &=& \varphi & \text{on } \Gamma, \end{array} \right.$$

  and $u_p = u_p(\varphi)$ the unique solution of

$$(\mathcal{P}_p) \left\{ \begin{array}{rcll} -\Delta u_p + (\beta^2 - n^2\,\omega^2)\, u_p &=& (n^2 - n_o^2)\,\omega^2\, u_i & \text{in } \Omega_i, \\ u_p &=& 0 & \text{on } \Gamma, \end{array} \right.$$

  which can be proved to exist for certain values of $\omega$ and $\beta$.

Then we define

$$S_e(\omega,\beta)\varphi = \left( \frac{\partial u_e^+}{\partial \mathbf{n}}\Big|_{\Gamma^+} , \frac{\partial u_e^-}{\partial \mathbf{n}}\Big|_{\Gamma^-} \right),$$

$$S_i(\omega,\beta)\,\varphi = \left( \frac{\partial u_i}{\partial \mathbf{n}}\Big|_{\Gamma^+} , \frac{\partial u_i}{\partial \mathbf{n}}\Big|_{\Gamma^-} \right), \tag{2.4}$$

$$S_p(\omega,\beta)\,\varphi = \left( \frac{\partial u_p}{\partial \mathbf{n}}\Big|_{\Gamma^+} , \frac{\partial u_p}{\partial \mathbf{n}}\Big|_{\Gamma^-} \right).$$

Problems $(\mathcal{P}_e)$ and $(\mathcal{P}_i)$ are coercive (see Theorem 3.1 and Theorem 3.3 in [11]) and thus uniquely solvable. They can be explicitly solved by using partial Fourier transform in the $x_1$ direction. This allows us to compute explicitly the symbols of the operators $S_e$ and $S_i$ and to show that they have a pure continuous spectrum. One can also show that the operator $S_e - S_i$ is an isomorphism. The existence and uniqueness of the solution of the problem $(\mathcal{P}_p)$ is not *a priori* obvious since, in general, the problem is no longer coercive. In [11, 9], it is shown that the problem $(\mathcal{P}_p)$ is well-posed if and only if $\omega \notin G_i(\beta)$, where $G_i(\beta)$ is a finite (possibly empty) set of *irregular frequencies* (such as those occurring with integral equations). These irregular frequencies can be characterized throught a problem set in the central layer $\Omega_i$ (see Lemma 3.3 in [11]). Thus, if $\omega \notin G_i(\beta)$, $S_p$, and thus $S$, is well defined.

We refer to [11, 9] for various properties of $S_i$, $S_e$ and $S_p$. In particular, it is explained that $S$ is not very easy to handle numerically, one of the reasons being that it has a continuous spectrum. That is why, according to [11, 9], we introduce the operator

$$\mathrm{K}(\omega,\beta) = (S_i - S_e)^{-1} S_p, \tag{2.5}$$

which is well defined as a linear operator in $\mathrm{L}^2(\Gamma)$. One shows that $\mathrm{K}(\omega,\beta)$ is a compact operator whose spectrum is purely discrete and consists of a countable infinity of real eigenvalues admitting 0 as unique accumulation point (see [11] for the proof).

The relationship between $S(\omega,\beta)$ and $\mathrm{K}(\omega,\beta)$ is simply (I denotes the identity operator)

$$S(\omega,\beta) = (S_i - S_e)\{\mathrm{I} + \mathrm{K}(\omega,\beta)\}, \tag{2.6}$$

so it is obvious that the problem $(\mathcal{P}_S)$ is equivalent to the following

$$(\mathcal{P}_{\mathrm{K}}) \left\{ \begin{array}{c} \textit{For a given } \beta\textit{, find } \omega > 0 \ (\omega \notin G_i(\beta)) \textit{ with } (\omega,\beta) \in E, \\ \textit{such that } -1 \textit{ is an eigenvalue of } \mathrm{K}(\omega,\beta), \end{array} \right.$$

or, equivalently,

$$\left\{ \begin{array}{c} \textit{For a given } \beta\textit{, find } \omega > 0 \ (\omega \notin G_i(\beta)) \textit{ with } (\omega,\beta) \in E\textit{, such that} \\ \textit{there exists } \varphi \in \mathrm{L}^2(\Gamma),\ \varphi \neq 0 \textit{ satisfying} \\ (\mathrm{I} + \mathrm{K}(\omega,\beta))\,\varphi = 0. \end{array} \right. \tag{2.7}$$

Thus, the algorithm for searching guided modes is:

1. Compute the eigenvalues $\lambda(\omega,\beta)$ of $\mathrm{K}(\omega,\beta)$.
2. Solve the equations $\lambda(\omega,\beta) = -1$ in the plane $(\omega,\beta)$.

The main difficulty is the computation of the eigenvalues of the operator $\mathrm{K}(\omega,\beta)$, which must be done numerically. This will be the object of sections 3, 4 and 5. The resolution of the dispersion equations $\lambda(\omega,\beta) = -1$ does not present any particular difficulty and it will be briefly explained in Section 6.

# 3 Numerical approximation of the problem $(\mathcal{P}_\mathrm{K})$

In this section, we sketch the main steps of the numerical approximation of the problem $(\mathcal{P}_\mathrm{K})$. We refer the reader to [11, 10] for more details and for the corresponding numerical analysis.

## 3.1 The truncation of $\Gamma$. Introducing the parameter R

The first difficulty one has to face for solving problem $(\mathcal{P}_\mathrm{K})$ lies in the fact that the unknown function $\varphi$ is defined in a one dimensional but unbounded domain, namely the boundary $\Gamma$. To avoid this difficulty, we propose a domain truncation procedure. The idea is working with functions defined on the bounded domain

$$\Gamma_\mathrm{R} = \Gamma \cap \{(x_1,x_2) \ / \ a^- - \mathrm{R} < x_1 < a^+ + \mathrm{R}\},$$

where $\mathrm{R} > 0$ is an approximation parameter devoted to tend to $+\infty$. We have denoted by $a^-$ and $a^+$ the abscises of two vertical lines $x_1 = a^-$ $(\Sigma^-)$ and $x_1 = a^+$ $(\Sigma^+)$ enclosing the perturbation $\mathcal{K}$. Moreover $\ell$ denotes the distance between $\mathcal{K}$ and these lines (see Fig. 4). We set $\widetilde{\Gamma}_\mathrm{R} = \Gamma \setminus \Gamma_\mathrm{R}$ and use the orthogonal decomposition

$$\mathrm{L}^2(\Gamma) = \mathrm{L}^2(\Gamma_\mathrm{R}) \oplus \mathrm{L}^2(\widetilde{\Gamma}_\mathrm{R}) \tag{3.1}$$

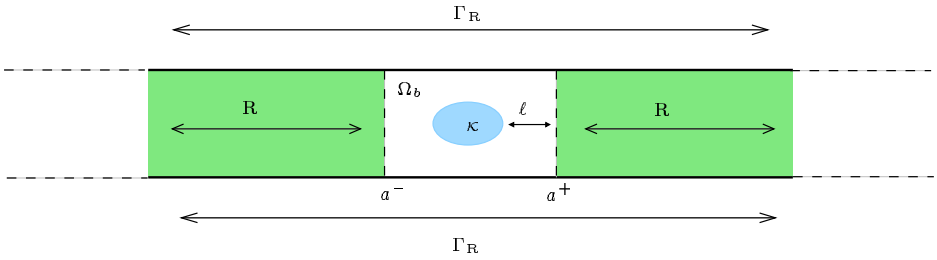


Figure 4: Truncation method.

where $L^2(\Gamma_R)$ (respectively $L^2(\widetilde{\Gamma}_R)$) denotes the subspace of functions in $L^2(\Gamma)$ whose support is included in $\Gamma_R$ (respectively $\widetilde{\Gamma}_R$).

We also introduce the orthogonal projector $\Pi_R$ on $L^2(\Gamma_R)$ defined by

$$\begin{array}{rccl} \Pi_R : & L^2(\Gamma) & \longrightarrow & L^2(\Gamma) \\ & \varphi & \longrightarrow & \Pi_R\varphi = \chi_R\,\varphi \end{array} \tag{3.2}$$

where $\chi_R$ denotes the characteristic function of $\Gamma_R$.

Now the idea is to write an equation for $\Pi_R\varphi$, the "restriction" of $\varphi$ to $\Gamma_R$. Such an equation does not exist but we can write an approximate equation, up to *exponentially* small errors, whose unknown $\varphi_R$ will be an approximation of $\Pi_R\varphi$.

By decomposing $\varphi$ as

$$\varphi = \Pi_R\varphi + (\varphi - \Pi_R\varphi)$$

and applying the operator $\Pi_R$ to (2.7), we obtain

$$\Pi_R\varphi + \Pi_R K\Pi_R\,\varphi + \Pi_R K(I - \Pi_R)\,\varphi = 0,$$

that we can rewrite as

$$\begin{array}{rcl} \Pi_R\varphi & + & \Pi_R\,(S_i - S_e)^{-1}\,\Pi_R\,S_p\,\Pi_R\,\varphi \\ & + & \{\,\Pi_R\,(S_i - S_e)^{-1}\,(I - \Pi_R)\,S_p\,\Pi_R \\ & + & \Pi_R\,(S_i - S_e)^{-1}\,S_p\,(I - \Pi_R)\,\}\,\varphi \;=\; 0. \end{array}$$

The following estimates have been proved in [11, 10]

$$\begin{aligned} \|S_p\,(I - \Pi_R)\|_{\mathcal{L}(L^2(\Gamma))} &\le C\,e^{-\xi_1 R}, \\ \|(I - \Pi_R)\,S_p\|_{\mathcal{L}(L^2(\Gamma))} &\le C\,e^{-\xi_1 R} \end{aligned} \tag{3.3}$$

where we also demonstrate that there exists $\gamma_* > 0$ independent of $(\omega, \beta)$, such that

$$\forall (\omega, \beta) \in E, \quad \xi_1(\omega, \beta) = (\pi^2/L^2 + \beta^2 - n_o^2\, \omega^2)^{1/2} \geq \gamma_* > 0.$$

This shows that the quality of the approximation will never deteriorate even at the neighborhood of thresholds.

Estimates (3.3) allow us to approximate the equation (2.7) by

$$\{\mathrm{I} + \mathrm{K_R}\}\varphi_{\mathrm{R}} = 0, \quad \varphi_{\mathrm{R}} \in \mathrm{L}^2(\Gamma_{\mathrm{R}}) \tag{3.4}$$

with

$$\mathrm{K_R} = \Pi_{\mathrm{R}}(S_i - S_e)^{-1}\Pi_{\mathrm{R}} S_p \Pi_{\mathrm{R}}, \tag{3.5}$$

and then $\varphi_{\mathrm{R}}$ will be an approximation of $\Pi_{\mathrm{R}}\varphi$.

The estimates (3.3) can be proved thanks to regularity and decay properties of the solution $u_p$ of the interior problem $(\mathcal{P}_p)$ (cf. (3.9)). They are important because they allow us to obtain exponential estimates for the rate of convergence of the eigenvalues of $\mathrm{K_R}$ to the eigenvalues of K. More precisely, we prove that the nonzero eigenvalues of $\mathrm{K_R}$ converge exponentially to the nonzero eigenvalues of K as R goes to infinity (see [11, 10] for details).

As we shall see in the next sections, the approximation of operator $\mathrm{K_R}$ will be derived from an analytical computation of the operator $(S_i - S_e)^{-1}$ and a numerical approximation of operator $S_p$.

## 3.2 Resolution of the problem $(\mathcal{P}_p)$

For the practical computation of the operator $\mathrm{K_R}$, a previous step is the resolution of the problem $(\mathcal{P}_p)$. This is a boundary value problem in the strip $\Omega_i$ whose right hand side has compact support included in $\mathcal{K}$. Problem $(\mathcal{P}_p)$ can be numerically solved by using a *localized finite element method* taking into account the fact that $u_p$ satisfies an homogeneous Dirichlet condition.

The idea is to formulate a problem equivalent (in a certain sense) to the initial one but set in a bounded domain, by using transparent boundary conditions. To do that, we use the vertical lines $\Sigma^+$ and $\Sigma^-$ as artificial boundaries to split $\Omega_i$ into a bounded subdomain $\Omega_b$, containing the perturbation, and another one, $\Omega_i \setminus \Omega_b$, where the refraction index is constant. Then two separate problems are considered: a problem in the subdomain $\Omega_b$ and another one in the subdomain $\Omega_i \setminus \Omega_b$ and we see that the whole problem in $\Omega_i$ is solved if the continuity of $u_p$ and its normal derivatives across the artificial boundaries is ensured.

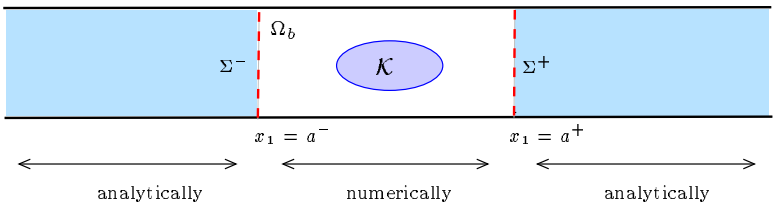


Figure 5: Computation of $u_p$.

The definition of these transparent boundary conditions involves the introduction of a Dirichlet to Neumman operator $T \in \mathcal{L}(\mathrm{H}_{00}^{1/2}(\Sigma^{\pm}), \mathrm{H}_{00}^{1/2}(\Sigma^{\pm})')$, depending on $(\omega, \beta)$, relating the trace of the solution on $\Sigma^{\pm}$ with the trace of its normal derivative. We have denoted by $\mathrm{H}_{00}^{1/2}(\Sigma^{\pm})$ the space

$$\mathrm{H}_{00}^{1/2}(\Sigma^{\pm}) = \{\varphi \in \mathrm{L}^2(\Sigma^{\pm}) / \sum_{k=1}^{\infty} |\varphi_k|^2 (1+k^2)^{1/2} < +\infty\}$$

and by $\mathrm{H}_{00}^{1/2}(\Sigma)'$ its topological dual.

This operator $T$ is known explicitly since the solution of the problem outside $\Omega_b$ can be obtained via a Fourier series expansion and is given by (see [11] for details)

$$[T(\omega,\beta)\varphi](x_2) = \sum_{k=1}^{\infty} \xi_k(\omega,\beta)\, \mathrm{w}_k(x_2)\, \varphi_k, \tag{3.6}$$

where $\{\mathrm{w}_k\}$ denotes the orthonormal basis of $\mathrm{H}_{00}^{1/2}([0,L])$ given by

$$\mathrm{w}_k(x_2) = (2/L)^{1/2} \sin(k\pi x_2/L), \quad k \geq 1, \tag{3.7}$$

$\varphi_k$ denotes the expansion coefficients of the function $\varphi$ in the basis $\{\mathrm{w}_k\}$ and

$$\xi_k = (k^2\pi^2/L^2 + \beta^2 - n_o^2\,\omega^2)^{1/2}, \quad k \in \mathbb{N}.$$

By using this operator $T$, we can write an equivalent formulation of the problem $(\mathcal{P}_p)$ which couples a variational formulation in the bounded domain $\Omega_b$ with a Fourier expansion outside. More precisely, the computation of $u_p$ has to be done in two steps:

- One computes $u_p$ inside $\Omega_b$ by solving numerically the boundary value problem

$$(\mathcal{P}_p^\Sigma) \quad \left\{ \begin{array}{rcll} -\Delta u_p + (\beta^2 - n^2\omega^2)\, u_p & = & (n^2 - n_o^2)\omega^2\, u_i & \text{in } \Omega_b\,, \ u_p \in \mathrm{H}^1(\Omega_b) \\ u_p & = & 0 & \text{on } \Gamma_b = \Gamma \cap \partial\Omega_b, \\ \dfrac{\partial u_p}{\partial \boldsymbol{\nu}} & = & -T u_p & \text{on } \Sigma^\pm\,. \end{array} \right. \tag{3.8}$$

  In (3.8), $\boldsymbol{\nu}$ denotes the outgoing normal vector to the boundaries $\Sigma^+$ or $\Sigma^-$.

- Knowing $u_p$ inside $\Omega_b$, we compute it analytically in the exterior domain $\Omega_i \backslash \Omega_b$ via the formulas

$$\begin{aligned} u_p(x_1, x_2) &= \sum_{k=1}^{\infty} u_k^+ \, \mathrm{w}_k(x_2)\, e^{-\xi_k(x_1 - a^+)} \quad \text{if } x_1 > a^+, \\ u_p(x_1, x_2) &= \sum_{k=1}^{\infty} u_k^- \, \mathrm{w}_k(x_2)\, e^{-\xi_k(a^- - x_1)} \quad \text{if } x_1 < a^-, \end{aligned} \tag{3.9}$$

  where $u_k^+$ and $u_k^-$ denotes the expansion coefficients in the basis $\{\mathrm{w}_k\}$ of the trace on $\Sigma^+$ and $\Sigma^-$ of the solution $u_p$ of $(\mathcal{P}_p^\Sigma)$.

## 3.3 Mixed formulation of $(\mathcal{P}_p^\Sigma)$

As a consequence of the definition (2.4), in order to compute the operator $S_p$ we must compute the trace of the normal derivative $\partial u_p / \partial \mathbf{n}$ on the boundary $\Gamma$. The main difficulty is to determine this trace on $\Gamma_b$ since on $\Gamma \backslash \Gamma_b$ it can be done explicitly from formulas (3.9).

It is well-known that for a numerical evaluation of the trace of the normal derivative of the solution of a second order elliptic problem, the use of mixed finite elements is particularly adapted. Indeed, the gradient of the solution is one of the unknowns of the problem and the trace of the normal derivative can be directly evaluated with the degrees of freedom of this unknown. That is why we now give a mixed formulation of the problem $(\mathcal{P}_p^\Sigma)$.

We introduce the vector function $\mathbf{p}$ defined in $\Omega_b$ by

$$\mathbf{p} = -\mathrm{grad}\, u_p. \tag{3.10}$$

Notice that $\mathbf{p}$ belongs to the space $\mathrm{H}(\mathrm{div}, \Omega_b)$ defined by

$$\mathrm{H}(\mathrm{div}, \Omega_b) = \{\mathbf{q} \in (\mathrm{L}^2(\Omega_b))^2 \ : \ \mathrm{div}\, \mathbf{q} \in \mathrm{L}^2(\Omega_b)\}.$$

Also we are led to rewrite the boundary conditions on $\Sigma^{\pm}$ in a different way. The idea is to consider the operator $B = T^{-1}$, the inverse of the operator $T$, given by

$$[B(\omega,\beta)\varphi](x_2) = \sum_{k=1}^{\infty} \xi_k^{-1}(\omega,\beta)\, \mathrm{w}_k(x_2)\, \varphi_k. \tag{3.11}$$

and to rewrite the boundary conditions on $\Sigma^+$ and $\Sigma^-$ as (see (3.8))

$$-B(\mathbf{p}\cdot\boldsymbol{\nu}) + u_p = 0. \tag{3.12}$$

Therefore, we rewrite the problem $(\mathcal{P}_p^{\Sigma})$ as a system of first order partial differential equations:

$$\left\{\begin{array}{l} \text{Find } \mathbf{p} \in \mathrm{H}(\mathrm{div},\Omega) \text{ and } u_p \in \mathrm{H}^1(\Omega_b) \text{ such that} \\ \qquad \begin{array}{rcll} \mathbf{p} + \mathrm{grad}\, u_p & = & 0 & \text{in } \Omega_b, \\ \mathrm{div}\, \mathbf{p} + \alpha\, u_p & = & f & \text{in } \Omega_b, \\ u_p & = & 0 & \text{on } \Gamma_b, \\ -B(\mathbf{p}\cdot\boldsymbol{\nu}) + u_p & = & 0 & \text{on } \Sigma^{\pm}, \end{array} \end{array}\right. \tag{3.13}$$

where we have denoted $f = (n^2 - n_o^2)\,\omega^2\, u_i$ and $\alpha = \beta^2 - n^2\omega^2$.

It is easy to prove that the the mixed variational formulation associated to (3.13), which permits to weaken the regularity of $u$ is

$$\left\{\begin{array}{l} \text{Find } \mathbf{p} \in Q \text{ and } u_p \in V \text{ such that} \\ \displaystyle\int_{\Omega_b} \mathbf{p}\cdot\mathbf{q} - \int_{\Omega_b} u_p\, \mathrm{div}\, \mathbf{q} + \int_{\Sigma^+} B(\mathbf{p}\cdot\boldsymbol{\nu})(\mathbf{q}\cdot\boldsymbol{\nu}) + \int_{\Sigma^-} B(\mathbf{p}\cdot\boldsymbol{\nu})(\mathbf{q}\cdot\boldsymbol{\nu}) = 0 \quad \forall \mathbf{q} \in Q \\ \displaystyle\int_{\Omega_b} \mathrm{div}\, \mathbf{p}\, v + \int_{\Omega_b} \alpha\, u_p\, v = \int_{\Omega_b} f\, v \quad \forall v \in V \end{array}\right. \tag{3.14}$$

where $V = \mathrm{L}^2(\Omega_b)$ and $Q = \mathrm{H}(\mathrm{div},\Omega_b)$.

**Remark 3.1** *Rigorously, the integrals* $\displaystyle\int_{\Sigma^{\pm}} B(\mathbf{p}\cdot\boldsymbol{\nu})(\mathbf{q}\cdot\boldsymbol{\nu})$ *must be understood as*

$$\langle B(\mathbf{p}\cdot\boldsymbol{\nu}), (\mathbf{q}\cdot\boldsymbol{\nu})\rangle_{\Sigma^{\pm}}$$

*where* $\langle\cdot,\cdot\rangle_{\Sigma^{\pm}}$ *denotes the duality pairing between* $\mathrm{H}_{00}^{1/2}(\Sigma^{\pm})'$ *and* $\mathrm{H}_{00}^{1/2}(\Sigma^{\pm})$.

### 3.4 The series truncation. Introducing the parameter $N$

From the numerical point of view, we must truncate both the series which appears in the expression of the operator $B$ and the series which defines the solution outside $\Omega_b$ at (large) rank $N$. Thus, in the domain $\Omega_b$, the solution $u_p$ of $(\mathcal{P}_p^\Sigma)$ will be approximated by the solution $u_p^N$ of the problem:

$$(\mathcal{P}_p^\Sigma)_N \left\{ \begin{array}{rcll} \mathbf{p}^N + \operatorname{grad} u_p^N & = & 0 & \text{in } \Omega_b, \quad u_p^N \in \mathrm{H}^1(\Omega_b) \\ \operatorname{div} \mathbf{p}^N + \alpha\, u_p^N & = & f & \text{in } \Omega_b, \\ u_p^N & = & 0 & \text{on } \Gamma_b, \\ -B^N(\mathbf{p}^N \cdot \boldsymbol{\nu}) + u_p^N & = & 0 & \text{on } \Sigma^\pm, \end{array} \right. \tag{3.15}$$

where $B^N$ denotes the operator obtained from (3.11) by truncation at rank N

$$[B^N(\omega,\beta)\varphi](x_2) = \sum_{k=1}^{N} \xi_k^{-1}(\omega,\beta)\, \mathrm{w}_k(x_2)\, \varphi_k. \tag{3.16}$$

In the exterior domain $\Omega_i \setminus \Omega_b$, $u_p^N$ can be expanded as (cf. [11] for details)

$$\begin{aligned} u_p^N(x_1,x_2) &= \sum_{k=1}^{N} (u_k^N)^+\, \mathrm{w}_k(x_2)\, e^{-\xi_k (x_1 - a^+)} \quad \text{if } x_1 > a^+, \\ u_p^N(x_1,x_2) &= \sum_{k=1}^{N} (u_k^N)^-\, \mathrm{w}_k(x_2)\, e^{-\xi_k (a^- - x_1)} \quad \text{if } x_1 < a^-. \end{aligned} \tag{3.17}$$

The reader will easily remark that $u_p^N$ is defined in such a way that

$$-\Delta u_p^N + (\beta^2 - n_{\mathrm{o}}^2\, \omega^2)\, u_p^N = 0 \quad \text{in } \Omega_i \setminus \Omega_b,$$

and such that $u_p^N$ is continuous across the two boundaries $\Sigma^\pm$. This is sufficient to define an approximation $S_p^N$ of the operator $S_p$ as follows

$$\left\{ \begin{array}{l} (S_p^N \varphi)_{|\Gamma_b} = \left. \dfrac{\partial u_p^N}{\partial \mathbf{n}} \right|_{\Gamma_b}, \\ (S_p^N \varphi)_{|\Gamma_{ext}} = \left. \dfrac{\partial u_p^N}{\partial \mathbf{n}} \right|_{\Gamma_{ext}}, \end{array} \right. \tag{3.18}$$

where we have denoted $\Gamma_{ext} = \Gamma \setminus \Gamma_b = \Gamma_{ext}^+ \cup \Gamma_{ext}^-$, with $\Gamma_{ext}^+ = \Gamma_{ext} \cap \Gamma^+$ and $\Gamma_{ext}^- = \Gamma_{ext} \cap \Gamma^-$. Moreover, according to formula (3.17), we have the following explicit representations of $(S_p^N \varphi)_{|_{\Gamma_{ext}^+}}$ :

$$\left\{ \begin{array}{rcll} (S_p^N \varphi)_{|_{\Gamma_{ext}^+}} & = & \displaystyle\sum_{k=1}^{N} (-1)^k \sqrt{\tfrac{2}{L}}\, \tfrac{k\pi}{L}\, (u_k^N)^+ e^{-\xi_k (x_1 - a^+)} & \text{if } x_1 > a^+, \\ (S_p^N \varphi)_{|_{\Gamma_{ext}^+}} & = & \displaystyle\sum_{k=1}^{N} (-1)^k \sqrt{\tfrac{2}{L}}\, \tfrac{k\pi}{L}\, (u_k^N)^- e^{-\xi_k (a^- - x_1)} & \text{if } x_1 < a^-, \end{array} \right. \tag{3.19}$$

and similar expressions on $\Gamma_{ext}^-$. In (3.19), $(u_k^N)^+$ and $(u_k^N)^-$ denote the expansion coefficients of the trace of $u_p^N|_{\Omega_b}$ on $\Sigma^+$ and $\Sigma^-$, in the basis $\{\mathrm{w}_k\}$.

This approximation of $S_p$ leads naturally to introduce the approximation $\mathrm{K}_{\mathrm{R}}^N$ of $\mathrm{K}_{\mathrm{R}}$ defined by

$$\mathrm{K}_{\mathrm{R}}^N(\omega,\beta) = (\Pi_{\mathrm{R}}\, (S_i - S_e)^{-1}\, \Pi_{\mathrm{R}})\, (\Pi_{\mathrm{R}}\, S_p^N\, \Pi_{\mathrm{R}}),$$

and then to consider the approximate problem

$$(\mathcal{P}_{\mathrm{K}_{\mathrm{R}}^N}) \left\{ \begin{array}{c} \textit{For a given } \beta, \textit{ find } \omega > 0, \omega \notin G_i(\beta) \textit{ with } (\omega,\beta) \in E, \\ \textit{such that } -1 \textit{ is an eigenvalue of } \mathrm{K}_{\mathrm{R}}^N(\omega,\beta). \end{array} \right.$$

The following result constitutes a theoretical justification of our method. Using the same method as in [11, 10], which concerns an analogous truncation procedure, one can show the

**Theorem 3.1** *Let $\lambda(\omega,\beta)$ be a nonzero eigenvalue of the operator $\mathrm{K}(\omega,\beta)$ with algebraic multiplicity $m$ and assume the ascent of $\lambda I - \mathrm{K}$ is $q \le m$. Then, there are $N_{\mathrm{o}} > 0$ and $\mathrm{R}_{\mathrm{o}} > 0$ such that, for $N > N_{\mathrm{o}}$ and $\mathrm{R} > \mathrm{R}_{\mathrm{o}}$ , there exist $\lambda_{N,\mathrm{R}}^1(\omega,\beta), \lambda_{N,\mathrm{R}}^2(\omega,\beta), \ldots, \lambda_{N,\mathrm{R}}^m(\omega,\beta)$ eigenvalues of $\mathrm{K}_{\mathrm{R}}^N(\omega,\beta)$ converging to $\lambda(\omega,\beta)$. Besides, we have the following estimate*

$$|\lambda(\omega,\beta) - \lambda_{N,\mathrm{R}}^j(\omega,\beta)| \le C_1\, N\, e^{-\pi\ell/L\, N/q} + C_2\, e^{-\xi_1\, \mathrm{R}/q}, \quad \textit{for } j = 1, \ldots, m.$$

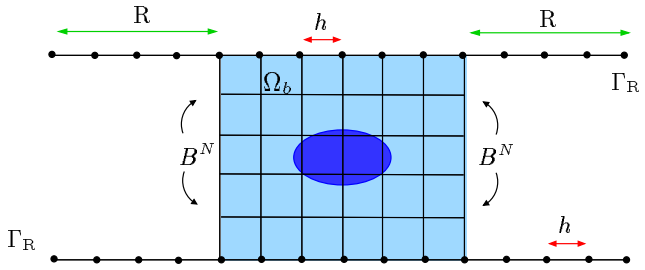


Figure 6: Parameters involved in the numerical method.

### 3.5 Discretization

In practice, one still cannot handle the operator $\mathrm{K}_{\mathrm{R}}^{N}$ numerically. We even need a discretization procedure involving:

- A finite element approximation for numerically solving the problem $(\mathcal{P}_p^{\Sigma})_N$, involving an approximation parameter $h$, which is the step-size of the mesh. This approximation, that will be done using the mixed-hybrid method described in Section 4, will produce a new approximate operator $S_p^{h,N}$ of $S_p^N$.
- The approximation of $\mathrm{L}^2(\Gamma_{\mathrm{R}})$ by a finite dimensional subspace (of piecewise constant functions, for instance) involving the same approximation parameter $h$.

These approximations lead to a new approximation of the operator $\mathrm{K}_{\mathrm{R}}^{N}(\omega,\beta)$, namely,

$$\mathrm{K}_{\mathrm{R}}^{h,N}(\omega,\beta) = (\Pi_{\mathrm{R}}\,(S_i - S_e)^{-1}\,\Pi_{\mathrm{R}})_h\,(\Pi_{\mathrm{R}}\,S_p^{h,N}\,\Pi_{\mathrm{R}})_h. \tag{3.20}$$

We summarize the meaning of the different parameters in Fig. 6. Finally, the numerical method consists in solving the problem

$$(\mathcal{P}_{\mathrm{K}_{\mathrm{R}}^{h,N}}) \left\{ \begin{array}{c} \textit{For a given } \beta\textit{, find } \omega > 0, \omega \notin G_i(\beta) \textit{ with } (\omega,\beta) \in E, \\ \textit{such that } -1 \textit{ is an eigenvalue of } \mathrm{K}_{\mathrm{R}}^{h,N}(\omega,\beta). \end{array} \right.$$

## 4 A mixed-hybrid finite element procedure to solve the problem $(\mathcal{P}_p^{\Sigma})_N$

In this section, we propose a mixed-hybrid finite element method for the numerical resolution of the problem $(\mathcal{P}_p^{\Sigma})_N$. To relieve the notation, we will suppress all the

subscripts $p$ and $N$ associated with the function $u_p^N$ (denoted $u$ in this section) and the other functions involved in the approximation procedure.

## 4.1 Discretized mixed formulation

In this paragraph, we approximate the solution of the problem

$$\left\{\begin{array}{l} \text{Find } \mathbf{p} \in Q \text{ and } u \in V \text{ such that} \\ \displaystyle\int_{\Omega_b} \mathbf{p}\cdot\mathbf{q} - \int_{\Omega_b} u \,\mathrm{div}\,\mathbf{q} + \int_{\Sigma^\pm} B^N(\mathbf{p}\cdot\boldsymbol{\nu})(\mathbf{q}\cdot\boldsymbol{\nu}) = 0 \quad \forall \mathbf{q} \in Q \\ \displaystyle\int_{\Omega_b} \mathrm{div}\,\mathbf{p}\, v + \int_{\Omega_b} \alpha\, u\, v = \int_{\Omega_b} f\, v \quad \forall v \in V, \end{array}\right. \tag{4.1}$$

which is obtained from (3.14) by replacing $B$ by $B^N$, by using a mixed finite element discretization.

Let $\mathcal{T}_h$ be a triangulation of $\bar{\Omega}_b$ made up of closed triangles $K$ with diameters bounded by $h$, satisfying the classical criteria for admissible triangulations. In the sequel, $\partial\mathcal{T}_h$ will denote the set of edges of the triangulation $\mathcal{T}_h$.

The function $u \in \mathrm{L}^2(\Omega_b)$ is approximated by a function $u_h$ constant per triangle:

$$u_h \in V_h \ = \{v_h \in \mathrm{L}^2(\Omega_b) \ : \ v_h|_K \in P_0(K) \ \forall\, K \in \mathcal{T}_h\},$$

where $P_0(K)$ is the space of constant functions on $K$. The degrees of freedom of functions in $V_h$ are their constant values on the triangles so the dimension of $V_h$ is the number of elements $\mathrm{N}_h^K$.

The vector field $\mathbf{p}$ is approximated by $\mathbf{p}_h$ using first order Raviart-Thomas finite elements:

$$\mathbf{p}_h \in Q_h = \left\{\mathbf{q}_h \in \mathrm{H}(\mathrm{div},\Omega) : \ \forall K \in \mathcal{T}_h, \ \mathbf{q}_h|_K(\mathbf{x}) = (a+dx_1, b+dx_2)\ , \ a,b,d \in \mathbb{R}\right\}.$$

The degrees of freedom for $\mathbf{p}_h$ are the values of the constant normal components, $\mathbf{p}_h\cdot\mathbf{n}$, on each edge of the triangles of the mesh so the dimension of $Q_h$ is the number of edges $N_h^e$.

Therefore the discrete version of (4.1) is

$$\left\{\begin{array}{l} \text{Find } \mathbf{p}_h \in Q_h \text{ and } u_h \in V_h \text{ such that} \\ \displaystyle\int_{\Omega_b} \mathbf{p}_h \cdot \mathbf{q}_h - \int_{\Omega_b} u_h \,\mathrm{div}\, \mathbf{q}_h = -\int_{\Sigma^\pm} B^N(\mathbf{p}_h \cdot \boldsymbol{\nu})(\mathbf{q}_h \cdot \boldsymbol{\nu}) \quad \forall \mathbf{q}_h \in Q_h, \\ \displaystyle\int_{\Omega_b} \mathrm{div}\, \mathbf{p}_h \, v_h + \int_{\Omega_b} \alpha \, u_h \, v_h = \int_{\Omega_b} f \, v_h \quad \forall v_h \in V_h. \end{array}\right. \tag{4.2}$$

The finite dimensional problem (4.2) is equivalent to solving a linear system of N equations in N unknowns, where $\mathrm{N} = \mathrm{N}_h^K + \mathrm{N}_h^e$. The matrix of this system is symmetric but it is not positive definite. This is a considerable source of trouble and, perhaps, the major drawback of the mixed approximation.

At this point, the hybridization plays an important role ([6, 18]). Mixed-hybrid finite element methods can be considered as a special class of mixed finite element methods which temporarily relax of the inter-element continuity condition. Such a trick involves the introduction of a suitable inter-element Lagrange multiplier $\lambda$ which has the effect of reducing (in the final system to be solved) the total number of unknowns. Besides it leads to solve a linear system for a matrix which is symmetric and positive definite instead of the original indefinite one.

## 4.2 Mixed-hybrid formulation

In this section we introduce a hybrid formulation of our problem. Instead of the space $Q_h$, we consider the space of discontinuous vector fields

$$\widetilde{Q}_h = \{\mathbf{q}_h \in (\mathrm{L}^2(\Omega_b))^2 : \ \mathbf{q}_h|_K = (\mathbf{x}) = (a + dx_1, b + dx_2)\,,\ a, b, d \in \mathbb{R}, \forall K \in \mathcal{T}_h\}.$$

The degrees of freedom of a function $\mathbf{p}_h \in \widetilde{Q}_h$ are the values of the normal components of $\mathbf{p}_h$ on the edges of $K$ and hence the dimension of $\widetilde{Q}_h$ is equal to $3 \times \mathrm{N}_h^K$.

To recover the continuity of $\mathbf{p}_h \cdot \mathbf{n}$ across edges, we introduce a Lagrange multiplier $\lambda_h$ and impose additional continuity equations. The Lagrange multiplier belongs to the discrete space

$$M_{h,0} = \left\{\mu_h \in L^2(\partial\mathcal{T}_h) : \ \mu_h|_e \in P_0(e),\ \forall e \in \partial\mathcal{T}_h,\ \mu_h|_e = 0,\ \forall e \in \partial\Omega_b\right\}, \tag{4.3}$$

where $P_0(e)$ is the space of constant functions defined on $e$, and the discrete **mixed-hybrid** variational formulation of problem (4.2) is the following (see [6, 18]):

$$\left\{\begin{array}{ll}
\text{Find } \mathbf{p}_h \in \widetilde{Q}_h,\, u_h \in V_h \text{ and } \lambda_h \in M_{h,0} \text{ such that} & \\
\displaystyle\sum_{K\in\mathcal{T}_h} \left\{ \int_K (\mathbf{p}_h \mathbf{q}_h - \operatorname{div} \mathbf{q}_h u_h) + \int_{\partial K\cap\Omega_b} \lambda_h \mathbf{q}_h\cdot\mathbf{n} \right\} = & \\
\displaystyle\sum_{K\in\mathcal{T}_h} - \int_{\partial K\cap\Sigma_\pm} B^N(\mathbf{p}_h\cdot\boldsymbol{\nu})(\mathbf{q}_h\cdot\boldsymbol{\nu}) & \forall \mathbf{q}_h \in \widetilde{Q}_h \\
\displaystyle\sum_{K\in\mathcal{T}_h} \left\{ \int_K \operatorname{div}\mathbf{p}_h v_h + \int_K \alpha\ u_h v_h \right\} = \sum_{K\in\mathcal{T}_h} \int_K f v_h & \forall v_h \in V_h \\
\displaystyle\sum_{K\in\mathcal{T}_h} \int_{\partial K} \mu_h \mathbf{p}_h\cdot\boldsymbol{\nu} = 0 & \forall \mu_h \in M_{h,0}
\end{array}\right. \tag{4.4}$$

Notice that it is the third equation which restores the continuity of the normal components of $\mathbf{p}_h$. One can show that (4.4) is equivalent to (4.1) and that $\lambda_h$ constitutes an approximation of the traces of $u$ on the interior edges of the mesh.

### 4.3 Matrix formulation

The advantage of the mixed-hybrid formulation comes from the fact that unknowns $\mathbf{p}_h$ and $u_h$ can be eliminated in such a way that the only unknown remaining in the domain $\Omega_b$ is $\lambda_h$. Moreover, for most of the degrees of freedom, this can be done by "static condensation" i.e. when the matrix and the right-hand side are assembled.

Let us be more precise and denote by

$$\begin{aligned}
\tilde{\mathbf{p}}_h &= \{(p_h\cdot\boldsymbol{\nu})\,(b_i)\} \ \in \mathbb{R}^{\,3\mathrm{N}_h^K},\\
\tilde{\mathbf{u}}_h &= \{u_h(a_K)\} \ \in \mathbb{R}^{\,\mathrm{N}_h^K},\\
\tilde{\boldsymbol{\lambda}}_h &= \{\lambda_h(b_i)\} \ \in \mathbb{R}^{\,\widetilde{\mathrm{N}}_h^e},
\end{aligned}$$

the vectors of degrees of freedom corresponding to the unknowns $\mathbf{p}_h$, $u_h$ and $\lambda_h$; $b_i$ denotes the middle point of the edge number $i$ of the triangulation, $a_K$ the baricenter of the element $K$, and we introduce $\widetilde{\mathrm{N}}_h^e$ as the number of edges on $\partial\mathcal{T}_h\cap\Omega_b$.

As usual, the matrices associated with the bilinear forms in the variational formulation are defined by

$$\begin{aligned}
\tilde{\mathbf{q}}_h^t \, \mathcal{A}_h \, \tilde{\mathbf{p}}_h &= \sum_{K \in \mathcal{T}_h} \left\{ \int_K \mathbf{p}_h \mathbf{q}_h + \int_{\partial K \cap \Sigma_\pm} B^N (\mathbf{p}_h \cdot \boldsymbol{\nu})(\mathbf{q}_h \cdot \boldsymbol{\nu}) \right\} \\
\tilde{\mathbf{u}}_h^t \, \mathcal{B}_{1h} \, \tilde{\mathbf{q}}_h &= \sum_{K \in \mathcal{T}_h} - \int_K \operatorname{div} \mathbf{q}_h u_h \\
\tilde{\mathbf{v}}_h^t \, \mathcal{B}_{2h} \, \tilde{\mathbf{u}}_h &= \sum_{K \in \mathcal{T}_h} \int_K \alpha \; u_h v_h \\
\tilde{\mathbf{q}}_h^t \, \mathcal{C}_h \, \tilde{\boldsymbol{\lambda}}_h &= \sum_{K \in \mathcal{T}_h} \int_{\partial K \cap \Omega_b} \lambda_h \mathbf{q}_h \cdot \mathbf{n}
\end{aligned} \tag{4.5}$$

Then the linear problem (4.4) is written in terms of these matrices as follows

$$\begin{bmatrix} \mathcal{A}_h & \mathcal{B}_{1h} & \mathcal{C}_h \\ \mathcal{B}_{1h}^t & \mathcal{B}_{2h} & 0 \\ \mathcal{C}_h^t & 0 & 0 \end{bmatrix} \begin{bmatrix} \tilde{\mathbf{p}}_h \\ \tilde{\mathbf{u}}_h \\ \tilde{\boldsymbol{\lambda}}_h \end{bmatrix} = \begin{bmatrix} \tilde{l}_{1h} \\ \tilde{l}_{2h} \\ \tilde{l}_{3h} \end{bmatrix} \tag{4.6}$$

where

$$\tilde{l}_{1h} = 0, \quad \tilde{\mathbf{v}}_h^t \, \tilde{l}_{2h} = \sum_{K \in \mathcal{T}_h} \int_K f v_h, \quad \tilde{l}_{3h} = 0.$$

Of course, we have increased the number of unknowns (from $\mathrm{N}_h^K + \mathrm{N}_h^e$ before hybridization to $4\mathrm{N}_h^K + \widetilde{\mathrm{N}}_h^e$ in (4.6)). However, it is possible to eliminate $\tilde{\mathbf{p}}_h$ and $\tilde{\mathbf{u}}_h$ and solve a system involving the variable $\tilde{\boldsymbol{\lambda}}_h$ only. This is essentially due to the fact that, if we except the effect of the boundary operator $B^N$, the matrices $\mathcal{A}_h$, $\mathcal{B}_{1h}$ and $\mathcal{B}_{2h}$ are purely local to an element, the only coupling between elements coming from the matrix $\mathcal{C}_h$.

Let us recall here the algebra of the procedure even if it is standard. Indeed, since $\mathcal{A}_h$ is a positive definite matrix, one can easily obtain $\tilde{\mathbf{p}}_h$ from the first equation of (4.6)

$$\tilde{\mathbf{p}}_h = \mathcal{A}_h^{-1}(\tilde{l}_{1h} - \mathcal{B}_{1h} \tilde{\mathbf{u}}_h - \mathcal{C}_h \tilde{\boldsymbol{\lambda}}_h).$$

Then (4.6) yields

$$\begin{bmatrix} \mathcal{B}_{2h} - \mathcal{B}_{1h}^t \mathcal{A}_h^{-1} \mathcal{B}_{1h} & -\mathcal{B}_{1h}^t \mathcal{A}_h^{-1} \mathcal{C}_h \\ -\mathcal{C}_h^t \mathcal{A}_h^{-1} \mathcal{B}_{1h} & -\mathcal{C}_h^t \mathcal{A}_h^{-1} \mathcal{C}_h \end{bmatrix} \begin{bmatrix} \tilde{\mathbf{u}}_h \\ \tilde{\boldsymbol{\lambda}}_h \end{bmatrix} = \begin{bmatrix} \tilde{l}_{2h} - \mathcal{B}_{1h}^t \mathcal{A}_h^{-1} \tilde{l}_{1h} \\ \tilde{l}_{3h} - \mathcal{C}_h^t \mathcal{A}_h^{-1} \tilde{l}_{1h} \end{bmatrix}. \tag{4.7}$$

Now, for $h$ small enough, it can be shown that the matrix $\mathcal{B}_{2h} - \mathcal{B}_{1h}^t \mathcal{A}_h^{-1} \mathcal{B}_{1h}$ is positive definite so we can eliminate $\tilde{u}_h$ in (4.7) by using the expression

$$\tilde{\mathbf{u}}_h = (\mathcal{B}_{2h} - \mathcal{B}_{1h}^t \mathcal{A}_h^{-1} \mathcal{B}_{1h})^{-1} (\tilde{l}_{2h} - \mathcal{B}_{1h}^t \mathcal{A}_h^{-1} \tilde{l}_{1h} + \mathcal{B}_{1h}^t \mathcal{A}_h^{-1} \mathcal{C}_h \boldsymbol{\lambda}_h)$$

obtained from the first equation. By doing so we are led to solve the following linear system, the unknown of which is only $\tilde{\lambda}_h$

$$\mathcal{D}_h \tilde{\boldsymbol{\lambda}}_h = \mathcal{F}_h \tag{4.8}$$

where

$$\mathcal{D}_h = \mathcal{C}_h^t [\mathcal{A}_h^{-1} \mathcal{B}_{1h} (\mathcal{B}_{2h} - \mathcal{B}_{1h}^t \mathcal{A}_h^{-1} \mathcal{B}_{1h})^{-1} \mathcal{B}_{1h}^t \mathcal{A}_h^{-1} + \mathcal{A}_h^{-1}] \mathcal{C}_h$$

and

$$\mathcal{F}_h = \mathcal{C}_h^t \mathcal{A}_h^{-1} [\tilde{l}_{1h} - \mathcal{B}_{1h} (\mathcal{B}_{2h} - \mathcal{B}_{1h}^t \mathcal{A}_h^{-1} \mathcal{B}_{1h})^{-1} (\tilde{l}_{2h} - \mathcal{B}_{1h}^t \mathcal{A}_h^{-1} \tilde{l}_{1h})] - \tilde{l}_{3h}.$$

In practice, we notice that, since vector fields in $\widetilde{Q}_h$ are discontinuous, the matrix $\mathcal{A}_h$ has a particular diagonal block structure. Suppose that we adopt a numbering of the degrees of freedom for $\mathbf{p}_h$ such that the degrees of freedom associated to the same triangle are successively numbered and such that the triangles are arranged in such a way that the $N^-$ triangles having an edge on $\Sigma^-$ are numbered first while the $N^+$ triangles having an edge on $\Sigma^+$ appear at the end of the list. Then, the matrix $\mathcal{A}_h$ has the block structure sketched in Fig. 7. The small blocks are dimension 3. Each of them is associated to an interior triangle (i.e. a triangle who has no edge either on $\Sigma^+$ or on $\Sigma^-$) and connect the degrees of freedom associated to this triangle. The two big blocks $\mathcal{A}^+$ and $\mathcal{A}^-$ are (essentially) full matrices of respective dimensions $3\mathrm{N}^+$ and $3\mathrm{N}^-$. The presence of these full blocks is a consequence of the non-local boundary condition (3.12) which relates all the degrees of freedom of $\mathbf{p}_h$ located on $\Sigma^\pm$.

On the other hand, the $\mathrm{N}_h^K \times \mathrm{N}_h^K$ matrix $\mathcal{B}_{2h}$ is diagonal and the $\mathrm{N}_h^K \times 3\mathrm{N}_h^K$ matrix $\mathcal{B}_{1h}$ has the structure in Fig. 8.

A consequence of these structures is that the symmetric matrix $\mathcal{D}_h$ is mainly sparse. Its structure is analogous to the one of $\mathcal{A}_h$. More precisely, any degree of

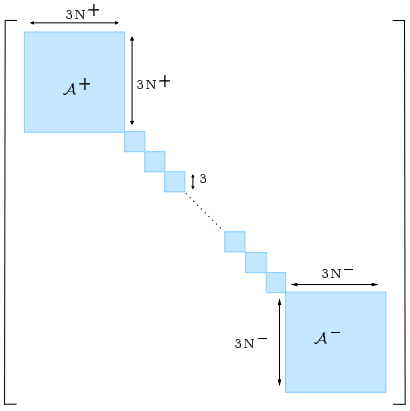


Figure 7: Structure of the matrix $\mathcal{A}_h$.

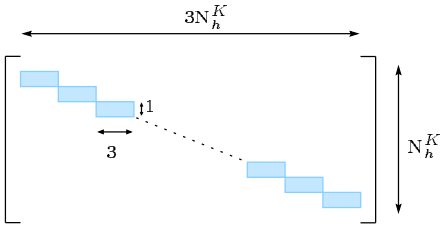


Figure 8: Structure of the matrix $\mathcal{B}_{1h}$.

freedom for $\lambda_h$ associated to an edge $e$ which is not connected to $\Sigma^+$ or $\Sigma^-$ is only connected to the four other edges of the two triangles which share $e$ as a common edge. However, all the edges connected to $\Sigma^-$ (respectively $\Sigma^+$) are connected, once again as a consequence of the non-local boundary condition.

# 5 Numerical approximation of the operator $\mathrm{K}(\omega, \beta)$

The aim of this section is to explain briefly how to construct the matrix which results from the numerical approximation of the operator $\mathrm{K}(\omega, \beta)$.

Although $\mathrm{K}(\omega, \beta)$ operates in $\mathrm{L}^2(\Gamma)$, after the truncation procedure described in Section 3.1, we shall only deal with functions with support in $\Gamma_\mathrm{R}$. Our objective will be then to define a finite dimensional subspace $\mathrm{Y}_{\mathrm{R},h}$ of $\mathrm{L}^2(\Gamma_\mathrm{R})$ to be precised, in which the operator $\mathrm{K}_\mathrm{R}^{h,N}(\omega, \beta)$, the numerical approximation of the operator $\mathrm{K}(\omega, \beta)$, will be defined. This is the object of §5.1 and §5.2.

The operator $\mathrm{K}_{\mathrm{R}}^{h,N}(\omega,\beta)$ will appear as the composition of two operators, $S_{p,\mathrm{R}}^{h,N}$ and $\mathrm{M}_{\mathrm{R}}^{h,N}$, both depending on $(\omega,\beta)$. Accordingly, the matrix $[\mathbb{K}_{\mathrm{R}}^{h,N}](\omega,\beta)$ associated with the operator $\mathrm{K}_{\mathrm{R}}^{h,N}(\omega,\beta)$ will be the product of the two matrices associated with the discrete operators $\mathrm{M}_{\mathrm{R}}^{h,N}$ and $S_{p,\mathrm{R}}^{h,N}$, i.e.

$$\left[\,\mathbb{K}_{\mathrm{R}}^{h,N}\,\right] = \left[\mathbb{M}_{\mathrm{R}}^{h,N}\right]\,\left[\mathbb{S}_{p,\mathrm{R}}^{h,N}\right].$$

The matrix $[\mathbb{M}_{\mathrm{R}}^{h,N}]$ is explicitly computed in §5.3. Finally, in §5.4, we explain how to compute the matrix $[\,\mathbb{S}_{p,\mathrm{R}}^{h,N}\,]$ associated with $S_{p,\mathrm{R}}^{h,N}$, the numerical approximation of operator $S_p$. We recall that the operator $\mathrm{K}_{\mathrm{R}}(\omega,\beta)$ appeared to be the product of two selfadjoint and compact operators, $(\Pi_{\mathrm{R}}\,(S_i - S_e)^{-1}\,\Pi_{\mathrm{R}})$ and $(\Pi_{\mathrm{R}}\,S_p^N\,\Pi_{\mathrm{R}})$ the former being strictly positive when restricted to $\mathrm{L}^2(\Gamma_{\mathrm{R}})$. Numerically this means that looking for the eigenvalues of $\mathrm{K}_{\mathrm{R}}^{h,N}$ leads, after discretization, to a standard symmetric generalized eigenvalue problem.

## 5.1 Construction of the approximation space

We introduce

$$\begin{aligned}\Gamma_{\mathrm{R}}^{+} &= \{(x_1,L)\,:\,a^- - \mathrm{R} < x_1 < a^+ + \mathrm{R}\},\\ \Gamma_{\mathrm{R}}^{-} &= \{(x_1,0)\,:\,a^- - \mathrm{R} < x_1 < a^+ + \mathrm{R}\}.\end{aligned}$$

Let us consider a uniform discretization $\mathcal{T}_h^{\Gamma_{\mathrm{R}}}$ of the interval $[a^- - \mathrm{R}, a^+ + \mathrm{R}]$ in $2\mathrm{J}+1$ segments of the same length $h$ as the step-size of the mesh of the domain $\Omega_b$ for the finite element procedure (see Fig. 5.1). For simplicity, we shall suppose without loss of generality that the abscises $a^-$ and $a^+$ which determines the boundaries $\Sigma^+$ and $\Sigma^-$ satisfy $a^- = -a^+$, with $a^+ > 0$.

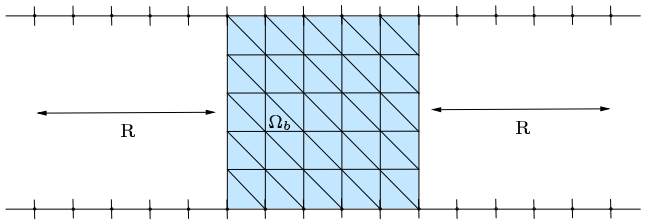


Figure 9: Discretization of the boundary $\Gamma_{\mathrm{R}}$ and the domain $\Omega_b$.

We shall denote by $\{\eta_{n-\frac{1}{2}}\}$ the set of $2\mathrm{J}+2$ discretization points, where each point is given by

$$\eta_{n-\frac{1}{2}} = \left(n - \frac{1}{2}\right) h, \quad -\mathrm{J} \leq n \leq \mathrm{J}+1.$$

Let $\mathrm{Y}_{\mathrm{R},h}$ be the approximation space of $\mathrm{L}^2(\Gamma_{\mathrm{R}}) = \mathrm{L}^2(\Gamma_{\mathrm{R}}^+) \times \mathrm{L}^2(\Gamma_{\mathrm{R}}^-)$ by $P_0$ finite elements defined as

$$\mathrm{Y}_{\mathrm{R},h} = \{\tau_h = (\tau_1^h, \tau_2^h)^t \in \mathrm{L}^2(\Gamma_{\mathrm{R}}) \ : \ \tau_i^h|_s \in P_0, \ i = 1,2 \ \ \forall s \in \mathcal{T}_h^{\Gamma_{\mathrm{R}}} \}.$$

For $-\mathrm{J} \leq n \leq \mathrm{J}$, let $\{\chi_n\}$ be the set of scalar functions defined as

$$\chi_n(x_1) = \begin{cases} \frac{1}{\sqrt{h}} & \text{if} \quad \eta_{n-\frac{1}{2}} \leq x_1 \leq \eta_{n+\frac{1}{2}}, \\ 0 & \text{otherwise.} \end{cases} \tag{5.1}$$

Then, a basis for $\mathrm{Y}_{\mathrm{R},h}$ is given by

$$B_{\mathrm{R},h} = \{\chi_n \, e_j, \ -\mathrm{J} \leq n \leq \mathrm{J}, \ 1 \leq j \leq 2\}, \tag{5.2}$$

where $\{e_1, e_2\}$ denotes the canonical basis of $\mathbb{R}^2$. We set $B_{\mathrm{R},h} = \{\varphi_l, \ 1 \leq l \leq 4\mathrm{J}+2\}$ where

$$\varphi_l = \chi_n e_i, \quad \text{with} \quad l = n + (i-1)(2\mathrm{J}+1) \tag{5.3}$$

in such a way that if $l \leq 2\mathrm{J}+1$, $\varphi_l$ has support in $\Gamma_{\mathrm{R}}^+$ and if $l \geq 2\mathrm{J}+2$, $\varphi_l$ has support in $\Gamma_{\mathrm{R}}^-$.

## 5.2 Definition of the operator $\mathrm{K}_{\mathrm{R}}^{h,N}(\omega,\beta)$

Let us consider the $\mathrm{L}^2$-projection operator

$$\begin{array}{rccc} \Pi_{\mathrm{R},h} : & \mathrm{L}^2(\Gamma) & \longrightarrow & \mathrm{Y}_{\mathrm{R},h} \\ & \phi & \longrightarrow & \phi_{\mathrm{R},h} \end{array}$$

where

$$\phi_{\mathrm{R},h}(x_1) = \frac{1}{h} \int_{\eta_{i-\frac{1}{2}}}^{\eta_{i+\frac{1}{2}}} \phi(s)\, ds, \quad \text{if} \ \ x_1 \in (\eta_{i+\frac{1}{2}}, \eta_{i-\frac{1}{2}}).$$

The adjoint $\Pi_{\mathrm{R},h}^*$ of $\Pi_{\mathrm{R},h}$ is explicitly given by

$$\begin{array}{rccc} \Pi_{\mathrm{R},h}^* : & \mathrm{Y}_{\mathrm{R},h} & \longrightarrow & \mathrm{L}^2(\Gamma) \\ & \phi_{\mathrm{R},h} & \longrightarrow & \phi \end{array}$$

where

$$\phi(x_1) = \begin{cases} 0 & \text{if} \quad x_1 \notin (-\mathrm{R}, \mathrm{R}) \\ \phi_{\mathrm{R},h}(x_1) & \text{otherwise.} \end{cases}$$

We define the operators

$$S^{h,N}_{p,\mathrm{R}} \;=\; \Pi_{\mathrm{R},h} \circ S^{h,N}_{p} \circ \Pi^{*}_{\mathrm{R},h} \tag{5.4}$$

and

$$\mathrm{M}^{h,N}_{\mathrm{R}} \;=\; \Pi_{\mathrm{R},h} \circ (S_i - S_e)^{-1} \circ \Pi^{*}_{\mathrm{R},h}. \tag{5.5}$$

Then, the operator $\mathrm{K}^{h,N}_{\mathrm{R}} : \mathrm{Y}_{\mathrm{R},h} \longrightarrow \mathrm{Y}_{\mathrm{R},h}$ that numerically approximates the operator K is defined as

$$\mathrm{K}^{h,N}_{\mathrm{R}} = \mathrm{M}^{h,N}_{\mathrm{R}} \circ S^{h,N}_{p,\mathrm{R}}.$$

Thus, the matrix $[\mathbb{K}^{h,N}_{\mathrm{R}}](\omega,\beta)$ representing the operator $\mathrm{K}^{h,N}_{\mathrm{R}}(\omega,\beta)$ in the basis $B_{\mathrm{R},h}$ will be the product of the two matrices associated with the discrete operators $\mathrm{M}^{h,N}_{\mathrm{R}}$ and $S^{h,N}_{p,\mathrm{R}}$, i.e.

$$\left[\, \mathbb{K}^{h,N}_{\mathrm{R}} \,\right] = \left[\mathbb{M}^{h,N}_{\mathrm{R}}\right] \left[\mathbb{S}^{h,N}_{p,\mathrm{R}}\right].$$

The computation of these matrices will be the object of the next two sections.

## 5.3 Computation and properties of $[\,\mathbb{M}^{h,N}_{\mathrm{R}}\,]$

The definition of the operator $\mathrm{M}^{h,N}_{\mathrm{R}}$ given by (5.5) involves the operator $(S_i - S_e)^{-1}$. As we have seen in [9], this operator can be analytically computed by Fourier transform in the $x_1$ space direction. For any $\phi, \psi \in \mathrm{L}^2(\Gamma)$, Plancherel's Lemma (cf. [5]), leads us to compute an integral of the type

$$((S_i - S_e)^{-1}(\omega,\beta)\,\phi, \psi) \;=\; \frac{1}{2\pi} \int_{\mathbb{R}} \widehat{\mathrm{M}}(\omega,\beta;k)\, \widehat{\phi}(k) \cdot \overline{\widehat{\psi}}(k)\; dk \tag{5.6}$$

where $k$ denotes the Fourier variable and $\widehat{\mathrm{M}}(\omega,\beta;k)$ is nothing but the symbol of the operator $(S_i - S_e)^{-1}$ in the Fourier domain. The matrix $[\mathrm{M}(\omega,\beta;k)]$ representing the operator $\widehat{\mathrm{M}}(\omega,\beta;k)$ can be computed analytically. Indeed, one has

$$[\mathrm{M}(\omega,\beta;k)] = (M_i - M_e)^{-1}(\omega,\beta;k)$$

where $M_e(\omega,\beta;k)$ and $M_i(\omega,\beta;k)$ represent the matrices associated to the operators $S_e(\omega,\beta)$ and $S_i(\omega,\beta)$ in the Fourier domain (cf. [11, 9]). Thus, the entries $\mathbf{M}_{ij}(\omega,\beta;k),\ i,j=1,2,$ of $[\mathrm{M}(\omega,\beta;k)]$ are given by

$$\begin{aligned}
\mathbf{M}_{11}(\omega,\beta;k) &= \frac{1}{\mathrm{D}}\left(\xi_{\mathrm{o}}\coth\left(\xi_{\mathrm{o}}L\right)+\xi_{\infty}^{-}\right)\\
\mathbf{M}_{12}(\omega,\beta;k) &= \frac{1}{\mathrm{D}}\,\frac{\xi_{\mathrm{o}}}{\sinh(\xi_{\mathrm{o}}L)}\\
\mathbf{M}_{21}(\omega,\beta;k) &= \mathbf{M}_{12}(\omega,\beta;k)\\
\mathbf{M}_{22}(\omega,\beta;k) &= \frac{1}{\mathrm{D}}\left(\xi_{\mathrm{o}}\coth(\xi_{\mathrm{o}}L)+\xi_{\infty}^{+}\right)
\end{aligned} \tag{5.7}$$

where

$$\mathrm{D}=\left[\xi_{\mathrm{o}}\coth(\xi_{\mathrm{o}}L)+\xi_{\infty}^{+}\right]\left[\xi_{\mathrm{o}}\coth(\xi_{\mathrm{o}}L)+\xi_{\infty}^{-}\right]-\frac{\xi_{\mathrm{o}}^{2}}{\sinh^{2}(\xi_{\mathrm{o}}L)}$$

and

$$\begin{aligned}
\xi_{\mathrm{o}} &= (k^2+\beta^2-n_{\mathrm{o}}^2\,\omega^2)^{1/2} \qquad \text{if} \quad k^2+\beta^2-n_{\mathrm{o}}^2\,\omega^2\geq 0,\\
\xi_{\mathrm{o}} &= (n_{\mathrm{o}}^2\,\omega^2-k^2-\beta^2)^{1/2} \qquad \text{if} \quad k^2+\beta^2-n_{\mathrm{o}}^2\,\omega^2< 0.
\end{aligned}$$

Finally,

$$\begin{aligned}
\xi_{\infty}^{+} &= (k^2+\beta^2-n_{\infty}^{+}\,\omega^2)^{1/2},\\
\xi_{\infty}^{-} &= (k^2+\beta^2-n_{\infty}^{-}\,\omega^2)^{1/2}.
\end{aligned}$$

which are always real numbers (cf. [9]). Notice that $\mathrm{D}=D(k)\neq 0\forall k$ because $(M_i-M_e)^{-1}(k)$ is an invertible matrix forall $k$ (cf. [11]).

Then, in the basis $B_{\mathrm{R},h}$, the matrix $[\mathbb{M}_{\mathrm{R}}^{h,N}]$ representing the operator $\mathrm{M}_{\mathrm{R}}^{h,N}$ has the following block structure

$$\left[\mathbb{M}_{\mathrm{R}}^{h,N}\right]=\frac{1}{2\pi}\begin{bmatrix}\left[\mathrm{M}_{\mathrm{R}}^{h,N}(\omega,\beta)\right]^{11} & \left[\mathrm{M}_{\mathrm{R}}^{h,N}(\omega,\beta)\right]^{12}\\ \left[\mathrm{M}_{\mathrm{R}}^{h,N}(\omega,\beta)\right]^{21} & \left[\mathrm{M}_{\mathrm{R}}^{h,N}(\omega,\beta)\right]^{22}\end{bmatrix}.$$

Each block $\left[\mathrm{M}_{\mathrm{R}}^{h,N}(\omega,\beta)\right]^{ij}$ has dimension $(2\mathrm{J}+1)\times(2\mathrm{J}+1)$ and their respective elements are given by the formula

$$[\mathrm{M}_{\mathrm{R}}^{h,N}(\omega,\beta)]_{m,n}^{ij}=\int_{\mathbb{R}}\mathbf{M}_{ij}(\omega,\beta;k)\,\widehat{\chi}_n\,\overline{\widehat{\chi}_m}\,dk \qquad -\mathrm{J}\leq m,n\leq\mathrm{J}, \tag{5.8}$$

where $\widehat{\chi}_n$, the Fourier transform of $\chi_n$, is given by ($i$ denotes the complex unit)

$$\widehat{\chi}_n(k) = \frac{1}{\sqrt{h}} \frac{2\exp(ik\mathrm{R})}{k} \exp(-iknh) \exp\left(i\frac{kh}{2}\right) \sin\left(\frac{kh}{2}\right).$$

This shows that, in particular, thanks to the choice of a uniform mesh of the interval $[a^- - \mathrm{R}, a^+ + \mathrm{R}]$, the matrices $[\mathrm{M}_{\mathrm{R}}^{h,N}(\omega,\beta)]^{ij}$ are real symmetric Toeplitz matrices, which means that we only have to calculate one element per diagonal, namely one of the integrals (we use the fact that $\mathbf{M}_{ij}(\omega,\beta;k)$ is an even function of $k$)

$$\mathrm{M}_{ij}(\omega,\beta;p) = \int_0^{+\infty} \mathbf{M}_{ij}(\omega,\beta;k) \frac{1}{h}\frac{4}{k^2} \cos(kph) \sin^2\left(\frac{kh}{2}\right) dk, \quad 0 \le p \le 2\mathrm{J} \qquad (5.9)$$

so that

$$[\mathrm{M}_{\mathrm{R}}^{h,N}(\omega,\beta)]_{m,n}^{ij} = \mathrm{M}_{ij}(\omega,\beta;m-n).$$

Note also that the blocks $[\mathrm{M}_{\mathrm{R}}^{h,N}(\omega,\beta)]^{12}$ and $[\mathrm{M}_{\mathrm{R}}^{h,N}(\omega,\beta)]^{21}$ are identical since $\mathbf{M}_{12}(\omega,\beta,k) = \mathbf{M}_{21}(\omega,\beta;k)$ (see (5.7)). These properties about the blocks also ensure the symmetry of the global matrix $[\mathbb{M}_{\mathrm{R}}^{h,N}]$, which is a full and real matrix.

To compute the integrals (5.9), we have chosen a particular software of the `QUADPACK` library (cf. [16]), which is a collection of `Fortran` programs for the numerical evaluation of integrals.

## 5.4 Construction of the matrix $[\mathbb{S}_{p,\mathrm{R}}^{h,N}]$

In this section we are concerned with the computation of the matrix $[\mathbb{S}_{p,\mathrm{R}}^{h,N}]$ associated with the operator $S_{p,\mathrm{R}}^{h,N}$.

Taking into account (5.4), the element $(S_{p,\mathrm{R}}^{h,N})_{ij}$ of the matrix $[\mathbb{S}_{p,\mathrm{R}}^{h,N}]$ is given by the formula (note that $\Pi_{\mathrm{R},h}^{*}\varphi_j = \varphi_j$)

$$(S_{p,\mathrm{R}}^{h,N})_{ij} = \int_{\mathbb{R}} S_p^{h,N}\, \varphi_j \cdot \varphi_i \, dx_1$$

The computation can be split into tree steps:

- **Step 1.** Computation of the functions $u_i(\varphi_j)$ solution of the problem $(\mathcal{P}_i)$ associated with the boundary condition $\varphi_j$.

Using the fact that $(\mathcal{P}_i)$ is invariant by translation and the fact that the mesh for $\Gamma_{\rm R}$ is uniform, one simply has to compute the two functions $u_i^+$ and $u_i^-$ defined by:

$$\left\{\begin{array}{rcll} -\Delta\, u_i^+ \;+\; (\beta^2 - n_{\rm o}^2\,\omega^2)\, u_i^+ &=& 0 & \text{in} \quad \Omega_i \\ u_i^+ &=& 0 & \text{on} \quad \Gamma_{\rm R}^- \\ u_i^+ &=& \chi_0 & \text{on} \quad \Gamma_{\rm R}^+ \end{array}\right.$$

$$\left\{\begin{array}{rcll} -\Delta\, u_i^- \;+\; (\beta^2 - n_{\rm o}^2\,\omega^2)\, u_i^- &=& 0 & \text{in} \quad \Omega_i \\ u_i^- &=& \chi_0 & \text{on} \quad \Gamma_{\rm R}^- \\ u_i^- &=& 0 & \text{on} \quad \Gamma_{\rm R}^+ \end{array}\right.$$

where $\chi_0$ is defined in (5.1).

By using partial Fourier transform in the $x_1$ direction these are analytically given by:

$$\begin{aligned} \widehat{u_i^+}(x_1, x_2) &= \widehat{\chi}_0(k)\, \frac{\sinh\left(\xi_{\rm o}(k)\, x_2\right)}{\sinh\left(\xi_{\rm o}(k)\, L\right)} \\ \widehat{u_i^-}(x_1, x_2) &= \widehat{\chi}_0(k)\, \frac{\sinh\left(\xi_{\rm o}(k)\, (L - x_2)\right)}{\sinh\left(\xi_{\rm o}(k)\, L\right)} \end{aligned}$$

where we have denoted

$$\xi_{\rm o}(k) = \left\{\begin{array}{ll} (k^2 + \beta^2 - n_{\rm o}^2\,\omega^2)^{1/2} & \text{if} \quad k^2 + \beta^2 - n_{\rm o}^2\,\omega^2 \geq 0, \\ i\,(n_{\rm o}^2\,\omega^2 - k^2 - \beta^2)^{1/2} & \text{if} \quad k^2 + \beta^2 - n_{\rm o}^2\,\omega^2 < 0. \end{array}\right.$$

Then:

- If $\varphi_l = \chi_n e_1$, $\quad u_i(\varphi_l)(x_1, x_2) = u_i^+(x_1 - nh, x_2)$.
- If $\varphi_l = \chi_n e_2$, $\quad u_i(\varphi_l)(x_1, x_2) = u_i^-(x_1 - nh, x_2)$.

- **Step 2.** Computation of $S_p^{h,N}(\varphi_j)$.

Knowing $u_i(\varphi_j)$, we compute for each $j$, an approximation to the solution of

$$(\mathcal{P}_p) \left\{\begin{array}{rcll} -\Delta\, u_p \;+\; (\beta^2 - n^2\;\omega^2)\, u_p &=& (n^2 - n_{\rm o}^2)\,\omega^2\, u_i(\varphi_j) & \text{in} \quad \Omega_i, \\ u_p &=& 0 & \text{on} \quad \Gamma, \end{array}\right.$$

using the hybrid method described in Section 4. We deduce and approximation of the trace of the normal derivative of $u_p$ on $\Gamma_{\mathrm{R}}$ by (we keep here the notation of Section 4):

$$\begin{cases} \left.\dfrac{\partial u_p}{\partial \mathbf{n}}\right|_{\Gamma_b} \simeq \mathbf{p}_h \cdot \mathbf{n} \\ \left.\dfrac{\partial u_p}{\partial \mathbf{n}}\right|_{\Gamma_{\mathrm{R}} \setminus \Gamma_b} \text{ is given by (3.17)} \end{cases}$$

- **Step 3.** Computation of the $j$th column of the matrix $S^{h,N}_{p,\mathrm{R}}$.

The approximation of $(\partial u_p/\partial \mathbf{n})|_{\Gamma_{\mathrm{R}}}$ obtained in Step 2 is piecewise constant on $[a^-, a^+]$ and equal to a sum of exponentials decaying outside (see Fig. 10). We take its $\mathrm{L}^2(\Gamma_{\mathrm{R}})$-projection on $\mathrm{Y}_{\mathrm{R},h}$ (see Fig. 11). This gives a piecewise constant function whose values constitute the $j$th colum vector of the matrix $S^{h,N}_{p,\mathrm{R}}$.

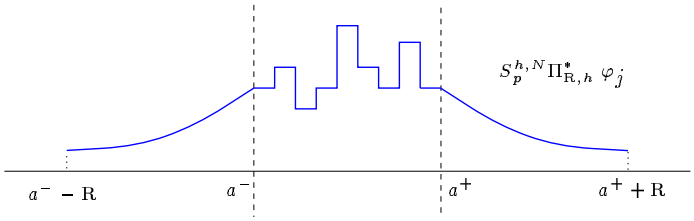


Figure 10: Approximation of $(\partial u_p/\partial \mathbf{n})|_{\Gamma_{\mathrm{R}}}$ after Step 2.

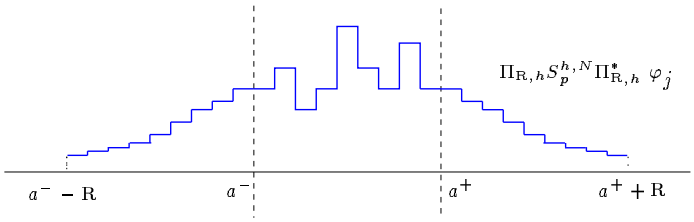


Figure 11: Approximation of $(\partial u_p/\partial \mathbf{n})|_{\Gamma_{\mathrm{R}}}$ after Step 3.

# 6 Numerical results

In this section, we present some numerical results obtained with a computer code implementing the method presented above.

## 6.1 The optical fiber test

The main purpose of this section is the validation of the method. To do that, we consider a step-index circular optical fiber whose core is a disk of radius 0.45 centered at $(0, 0.5)$ (see Fig. 12). The refraction index is $n_+ = 1.7$ in the core and $n_\infty = 1$ in the cladding. Notice that the search for guided modes in this example is a particular case of our problem where the stratified reference medium is in fact homogeneous ($n_\circ = n_\infty^+ = n_\infty^- = 1$) and the perturbation $\mathcal{K}$ is a circle of radius 0.45.

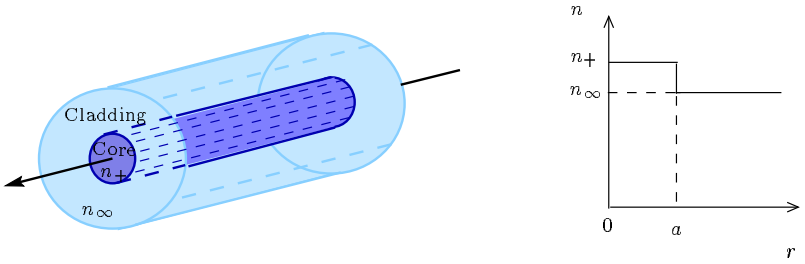


Figure 12: Step-index circular optical fiber and the corresponding refractive index variation.

The interest of this test lies in the fact that the guided modes can be computed analytically by using the method of separation of variables in polar coordinates $(r, \theta)$. Indeed, one can show that the guided modes are of the form

$$u_m(r)\exp(\pm im\theta), \quad m \in \mathbb{N}$$

where, for each $m$, the corresponding dispersion relation between $\omega$ and $\beta$ has an analytical formula (even though it still has to be solved numerically) in terms of Bessel functions given by (cf. [15, 17])

$$\kappa_\infty \frac{K_m'(0.45\,\kappa_\infty)}{K_m(0.45\,\kappa_\infty)} = \kappa \frac{J_m'(0.45\,\kappa)}{J_m(0.45\,\kappa)}. \tag{6.1}$$

In (6.1), $J_m$ (respectively $K_m$) denotes the Bessel (respectively the modified Bessel) function of first (respectively second) kind (cf. [1]), and where we have denoted

$$\kappa_\infty = \sqrt{\beta^2 - n_\infty^2\omega^2}, \quad \kappa = \sqrt{n_+^2\omega^2 - \beta^2}.$$

Table 1: Reference solutions of equation (6.1). We call "exact" the values obtained by solving numerically equation (6.1) and approximate those obtained from our numerical method.

| $\beta$ | $N(\beta)$ | m | $\omega(\beta)$ ("exact") | $\omega(\beta)$ (approximate) |
|---|---|---|---|---|
| 1.5 | 1 | 0 | 1.4711 | 1.4720 |
| 2 | 1 | 0 | 1.8534 | 1.8546 |
| 3 | 1 | 0 | 2.4874 | 2.4833 |
| 4 | 3 | 0 | 3.0534 | 3.0553 |
| | | 1 | 3.9661 | 3.9679 |
| | | | | 3.9728 |
| 4.5 | 3 | 0 | 3.3323 | 3.3344 |
| | | 1 | 4.2617 | 4.2634 |
| | | | | 4.2699 |
| 6 | 3 | 0 | 4.1616 | 4.1642 |
| | | 1 | 5.0510 | 5.0535 |
| | | | | 5.0610 |
| 6.5 | 6 | 0 | 4.4378 | 4.4404 |
| | | 1 | 5.3073 | 5.3098 |
| | | | | 5.3176 |
| | | 2 | 6.3458 | 6.3543 |
| | | | | 6.3597 |
| | | 0 | 6.4709 | 6.4768 |
| 7 | 6 | 0 | 4.7150 | 4.7170 |
| | | 1 | 5.5633 | 5.5660 |
| | | | | 5.5738 |
| | | 2 | 6.5861 | 6.5954 |
| | | | | 6.6002 |
| | | 0 | 6.7834 | 6.7917 |

In particular, we notice that, for $m \neq 0$ all the modes are double.

In order to obtain a reference solution, we have solved numerically equation (6.1). We give in Table 1 this "exact" solution for some values of $\beta$, which have been

specified in the first column. In the second column, we give the number of guided modes existing for each value of $\beta$ (counting with multiplicity) while in column three we have indicated the value of $m$ for which the frequencies associated with a guided mode detailed in column four have been obtained.

Table 2: Eigenvalues of the operator $\mathrm{K}_{\mathrm{R}}^{h,N}$. $h = 1/33$, $N = 100$

| R=1 | R=2 | R=3 |
|---|---|---|
| -0.99518017 | -0.998990380 | -0.999069840 |

Table 3: Eigenvalues of the operator $\mathrm{K}_{\mathrm{R}}^{h,N}$. $h = 1/33$, R = 3

| $N$=3 | $N$=30 | $N$=100 |
|---|---|---|
| -0.992325383 | -0.992344541 | -0.999069840 |

Table 4: Eigenvalues of the operator $\mathrm{K}_{\mathrm{R}}^{h,N}$. $N = 100$, R = 3

| $h$=1/11 | $h$=1/33 |
|---|---|
| -0.998479634 | -0.999069840 |

**A first validation test** For all the computations in this section, we choose $a^- = -0.5$ and $a^+ = 0.5$ which corresponds to a distance between the core of the fiber and the artificial vertical boundaries $\ell = 0.05$, which is quite small. The position of the two (artificial) horizontal boundaries $\Gamma_-$ and $\Gamma_-$ corresponds to $x_2 = 0$ and $x_2 = 1$ so the computational domain $\Omega_b$ for the finite element method is a square of side 1.

A first test to validate our method consists in considering a pair $(\omega, \beta)$ associated with a guided mode (this pair $(\omega, \beta)$ obtained from the dispersion relation (6.1)),

computing the eigenvalues of operator $\mathrm{K}_{\mathrm{R}}^{h,N}(\omega,\beta)$ given by (3.20) and verifying if $-1$ is one of them. We have taken $\beta = 2$, $\omega = 1.85$ (see Table 1). In the tables 2, 3 and 4, we have reported the eigenvalue of $\mathrm{K}_{\mathrm{R}}^{h,N}(\omega,\beta)$ which is closest to $-1$ for different values of $h$, $N$ and R in order to show the influence of these parameters in the numerical procedure. As expected, the lowest the step-size $h$ and higher the parameters R and $N$, the better the results.

**Finding the frequency for a given wavenumber** For such a computation, it is useful to consider the new unknown $\mathsf{v} = \omega/\beta$ —which is nothing but the phase velocity— because it varies in the fixed (i.e. independent of $\beta$) interval $(1/n_+, 1/n_\infty)$.

In Figure 13, we represent the variations of the functions $\mathsf{v} \longrightarrow \lambda_m^{h,N,R}(\beta\mathsf{v},\beta)$, for $\beta = 2$ and $m = 1,\ldots,4$. The fact that these curves seem to accumulate near 0 for large $m$ is in agreement with the fact that $\mathrm{K}(\omega,\beta)$ is a compact operator. On the other hand, the existence of an intersection point between the lowest curves and the line $\mathsf{y} = -1$ reveals the existence of a guided mode which is associated to $m = 1$ and whose phase velocity is closed to $1/n_\infty$. The vertical segment corresponds to the "exact" velocity of the mode $\mathsf{v} = 1.8534/2 = 0.9267$. The good agreement between the numerical solution and the "exact" one illustrates the efficiency of our method.

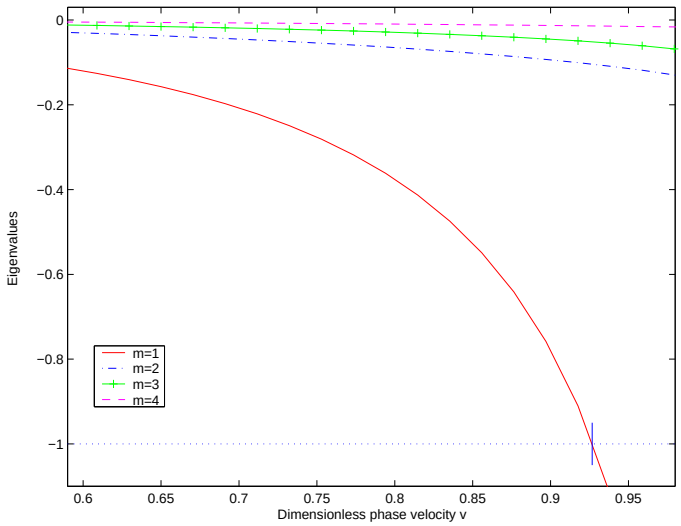


Figure 13: Case $\beta = 2$. Variation of the eigenvalue curves $\lambda_m(\beta\mathsf{v},\beta)$, $m = 1,\ldots,4$.

**Computing the dispersion curves** The solutions of equation (6.1) describe curves in the $(\omega, \beta)$ plane called *dispersion curves*. Each point on a dispersion curve represents a pair $(\omega, \beta)$ associated to a guided mode. They show, for each of the guided waves, the evolution of $\omega$ when $\beta$ varies. To recover numerically such dispersion curves, we use an algorithm with two steps for each value of $\beta$:

- **Step 1:** Computation of the eigenvalues $\lambda_m^{h,N,\mathrm{R}}(\beta\,\mathsf{v}, \beta)$, $m \geq 0$ of the operator $\mathrm{K}_{\mathrm{R}}^{h,N}(\omega, \beta)$, for $\beta$ given and $\omega$ satisfying $\beta^2/n_+^2 < \omega^2 < \beta^2/n_\infty^2$.
- **Step 2:** Resolution of the equations in $\mathsf{v}$

$$\lambda_m^{h,N,\mathrm{R}}(\beta\,\mathsf{v}, \beta) = -1, \quad \frac{1}{n_+} < \mathsf{v} < \frac{1}{n_\infty}, \quad m = 1, 2, \ldots, m(h). \tag{6.2}$$

For each equation, we have chosen to use a fixed point algorithm which is a variant of the secant method, called Illinois algorithm, which accelerates the convergence (see, for instance, [7]). To get the dispersion curves $\beta \longrightarrow \omega(\beta)$, this method can be coupled with a continuation method with respect to $\beta$ [12]. The idea is to use at the step $\beta = \beta_i$ the results obtained at the step $\beta = \beta_{i-1}$ by considering that, at the step $\beta = \beta_i$, an approximate value of $\omega_j(\beta_i)$ is given by $\omega_j(\beta_{i-1})$.

The computations we present here have been performed with $h = 1/33$ (this corresponds to 2178 triangles and 3333 degrees of freedom for $\lambda_h$ in the finite element method), $\mathrm{R} = 1$ and $N = 100$. The size of the matrix $\mathrm{K}_{\mathrm{R}}^{h,N}(\omega, \beta)$ is 198. The numerical results obtained have been detailed in column five of Table 1. We observe that the guided modes are computed with an accuracy better than $10^{-3}$.

In Figure 14, we have plotted the numerical dispersion curves (the variations of the frequency as a function of the wavenumber) for the five first modes. In fact, we have plotted seven curves since the second and the third ones are double. The computations have been made with $\Delta\beta = 0.5$ between two successive wavenumbers. We have also plotted the two curves $\beta \longrightarrow \beta/n_+$ and $\beta \longrightarrow \beta/n_\infty$ which enclose all the dispersion curves.

In Figure 15, we superpose the exact and approximate dispersion curves for the first three modes. The result is very good: we do not distinguish the exact curve from the numerical one. Moreover, the accuracy appears to be preserved even when one approaches a cut off frequency, as we expected from the theory. We emphasize this in the next paragraph.

**Guided modes close to the cut-off values** To check the numerical method in a limit situation like that of being close to the cut-off values, we run the code for

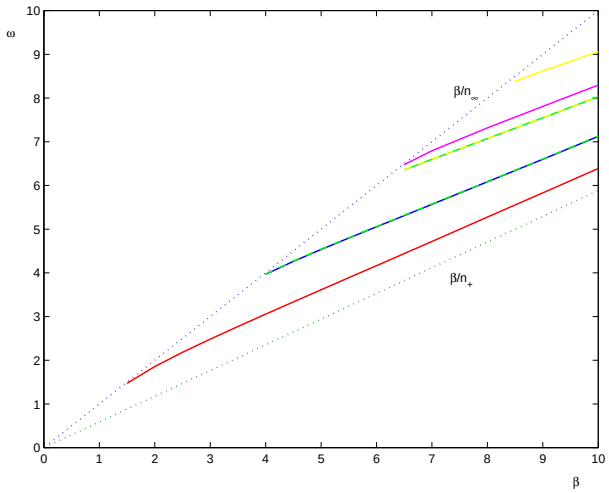


Figure 14: The numerical dispersion curves.

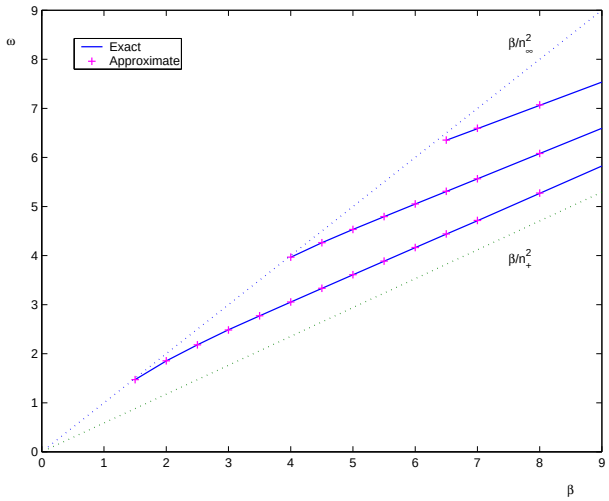


Figure 15: Comparison between "analytical" and numerical dispersion curves

$\beta = 3.98$, $\beta = 3.99$ and $\beta = 4$, since we have detected the presence of a cut-off value in the interval $[3.86, 3.90]$ (interval for $\beta$). In Table 5, we show the exact values

obtained from the dispersion relation and those obtained with our code. We have also included the value of $m$ for which the mode is obtained.

We can observe that the results we obtain agree with the expected ones except for the case $\beta = 3.9$. The exact mode corresponding to $m = 1$ is double. This mode has associated two different numerical modes but with the code we compute only one. This is due to the fact that each of these numerical modes correspond with a different cut-off value, i.e, one of the numerical modes has a cut-off value between [3.8,3.9] and the other one in the interval [3.9,4], while the exact cut-off value belongs to the interval [3.8,3.9]

Table 5: Guided modes close to the cutt-off values

| $\beta$ | m | "exact" value | approximate value $\omega$ | $\omega/\beta$ |
|---|---|---|---|---|
| 3.8 | 0 | 2.9410 | 2.9429 | 0.7744 |
| 3.9 | 0 | 2.9973 | 2.9992 | 0.7690 |
| | 1 | 3.8971 | 3.8976 | 0.9994 |
| 4 | 0 | 3.0534 | 3.0553 | 0.7638 |
| | 1 | 3.9661 | 3.9679 | 0.9919 |
| | | | 3.9728 | 0.9932 |

## 6.2 The integrated optics test

In this section, we study a less academic example in integrated optics. In this case analytical solutions are not available and that is why we have chosen to compare two numerical solutions: the one obtained with our method and the one obtained with the method proposed by Mahé in [14]. Contrary to the optical fiber test, we do not know the lower bound of the essential spectrum $\sigma_e(\beta)$.

Figure 16 represents an sketch of the cross section of the guide. The refraction index profile is given by

$$n(x_1, x_2) = \begin{cases} 3.17 & \text{if } x_2 > 1.5 \\ 1 & \text{if } x_2 < 0 \\ 3.44 & \text{if } (x_1, x_2) \in (-1, 1) \times (0.25, 1.25), \\ 3.38 & \text{otherwise} \end{cases}$$

In Table 6, we make a comparison between the results obtained from Mahé's method and the ones obtained with our method.

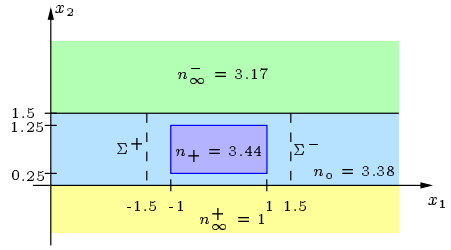


Figure 16: Cross section of the integrated optics waveguide test.

Table 6: Integrated optics test

| $\omega$ (Mahé's method ) | $\beta$ | $\omega$ (Our method) |
|---|---|---|
| 2 | 6.6394 | 2.0015 |
| 4 | 13.5730 | 3.9924 |
| 5 | 17.0329 | 4.9935 |
| | 16.8027 | 4.9270 |
| | 16.9174 | 4.9601 |
| 6 | 20.4885 | 5.9989 |
| | 20.3807 | 5.9920 |
| 7 | 23.9405 | 6.9988 |
| | 23.8404 | 6.9864 |
| | 23.6852 | 6.9698 |

In his method, Mahé takes the frequency as a parameter and he computes the wavenumber. In the second column of the table, we have represented the wavenumber, computed with Mahé's method, for different values of the frequency written in the first column. Taking this wavenumber as a parameter, we have computed, with our method, the values of the frequency associated to a guided mode and we have represented them in the third column. The obtained results coincide with those of Mahé.

Finally, in Fig. 18, we have plotted the second guided mode associated to $\beta = 23.3388$ and $\omega = 7$, and the third guided mode associated to $\beta = 23.18$ and $\omega = 7$, respectively.

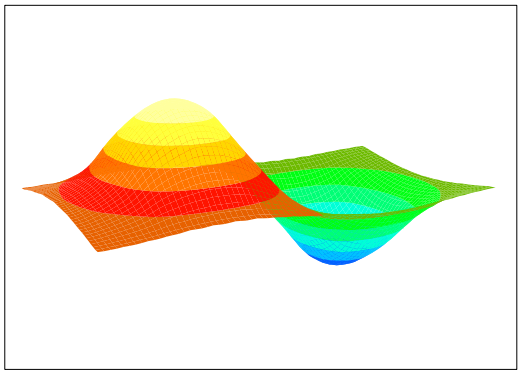

Figure 17: Second guided mode for $\beta = 23.84, \omega = 7$.

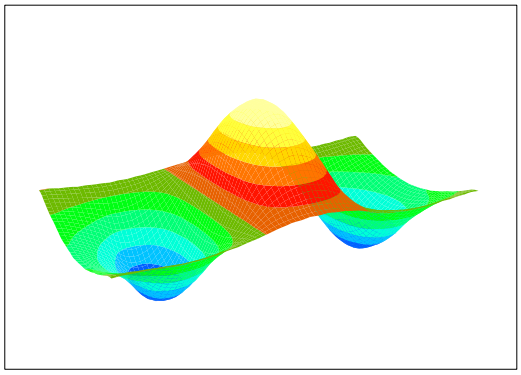

Figure 18: Third guided mode for $\beta = 23.68, \omega = 7$.

**Acknowledgment**

The authors thank F. Mahé for providing the results corresponding to the integrated optics test.

## References

[1] M. Abramowitz and I. Stegun. *Handbook of mathematical functions.* Dover Publication, 1968.

[2] A. S. Bonnet Ben Dhia. Analyse mathématique de la propagation de modes guidés dans les fibres optiques. Technical Report 229, Ecole Nationale Supérieure de Techniques Avancées, 1989.

[3] A. S. Bonnet Ben Dhia, G. Caloz, and F. Mahé. Guided modes of integrated optical guides. a mathematical study. *IMA Journal of Applied Mathematics*, 60, (1998), pp. 225–261.

[4] A. S. Bonnet Ben Dhia and F. Mahé. A guided mode in the range of the radiation modes for a rib waveguide. *J. Opt.*, 28, (1997), pp. 41–43.

[5] H. Brezis. *Analyse fonctionnelle. Théorie et applications.* Masson, 1983.

[6] F. Brezzi and M. Fortin. *Mixed and Hybrid Finite Element Methods.* Springer Series in Computational Mathematics. Springer-Verlag, Berlin [etc.], 1983.

[7] G. Dahlquist and A. Björck. *Numerical Methods.* Prentice-Hall, 1974.

[8] D. Givoli and J. B. Keller. Exact nonreflecting boundary conditions. *J. Computational Phys.*, 82, (1989), pp. 172–192.

[9] D. Gómez Pedreira and P. Joly. A method for computing guided waves in integrated optics. Part 1: Mathematical analysis. Accepted for publication in *SIAM J. Numer. Anal.*.

[10] D. Gómez Pedreira and P. Joly. A method for computing guided waves in integrated optics. Part 2: Numerical approximation. Submitted.

[11] D. Gómez Pedreira and P. Joly. Mathematical analysis of a method to compute guided waves in integrated optics. Technical Report 3933, Institut National de Recherche en Informatique et Automatique (I.N.R.I.A), May 2000.

[12] M. D. Gómez Pedreira. *A numerical method for the computation of guided waves in integrated optics.* PhD thesis, Universidad de Santiago de Compostela, 1999.

[13] P. Joly and C. Poirier. Mathematical analysis of electromagnetic open waveguides. *RAIRO Modél. Math. Anal. Numér.*, 29, (1995), pp. 505–575.

[14] F. Mahé. *Etude Mathématique et numérique de la propagation d'ondes electromagnétiques dans les microguides de l'optique intégrée.* PhD, Université de Rennes I, 1993.

[15] D. Marcuse. *Theory of dielectric optical waveguides.* Academic Press, 1974.

[16] R. Piessens and E. Donckert-Kapenga. QUADPACK, *A subroutine package for automatic integration.* Springer Series in Computational Mathematics. Springer-Verlag, Berlin [etc.], 1980.

[17] J. P. Pocholle. Caractéristiques de la propagation guidée dans les fibres optiques monomodes. Technical report, Thomson-CSF, 1983. Revue Technique 14.

[18] J. E. Roberts and J. M. Thomas. *Mixed and hybrid finite element methods*, volume **2**: Finite Element Methods of *Handbook of Numerical Analysis*, pages 523–639. Elsevier Science Publishing Co., 1991.

[19] C. Vassallo. *Optical Waveguide Concepts.* Elsevier Science Publishing Co., North Holland, 1991.

Unit´e de recherche INRIA Lorraine, Technopôle de Nancy-Brabois, Campus scientifique,
615 rue du Jardin Botanique, BP 101, 54600 VILLERS LÈS NANCY
Unit´e de recherche INRIA Rennes, Irisa, Campus universitaire de Beaulieu, 35042 RENNES Cedex
Unit´e de recherche INRIA Rhône-Alpes, 655, avenue de l'Europe, 38330 MONTBONNOT ST MARTIN
Unit´e de recherche INRIA Rocquencourt, Domaine de Voluceau, Rocquencourt, BP 105, 78153 LE CHESNAY Cedex
Unit´e de recherche INRIA Sophia-Antipolis, 2004 route des Lucioles, BP 93, 06902 SOPHIA-ANTIPOLIS Cedex

Éditeur
INRIA, Domaine de Voluceau, Rocquencourt, BP 105, 78153 LE CHESNAY Cedex (France)
http://www.inria.fr
ISSN 0249-6399